Research Article

Wedad Albalawi, Carlos A. Fotsing, Camus G. L. Tiofack*, Alim, Alidou Mohamadou, Rania A. Alharbey, and Samir A. El-Tantawy*

Nonlinear dynamics of the dissipative ionacoustic solitary waves in anisotropic rotating magnetoplasmas

https://doi.org/10.1515/phys-2025-0209 received March 28, 2025; accepted July 01, 2025

Abstract: This study explores the nonlinear dynamics of ion-acoustic waves (IAWs) in a magnetized, collisional, anisotropic rotating plasma that includes hot ions, superthermal electrons, and positrons. Anisotropic ion pressure is defined using the Chew-Goldberger-Low theory. Our linear analysis shows that pressure anisotropy notably impacts wave frequency, particularly for shorter wavelengths, and identifies a threshold wavenumber beyond which wave propagation is impossible. We derive a nonlinear damped Zakharov-Kuznetsov equation by applying the reductive perturbation technique. This equation describes the phase velocity and profile of ion-acoustic solitary waves, which are significantly influenced by superthermal, electron-positron temperature ratio, pressure anisotropy, the Coriolis force, and ion collisions. Our numerical analysis reveals that IAWs propagate in the plasma in a direction parallel to the magnetic field with a phase velocity that is unaffected by the plasma rotation frequency Ω_0 , the magnetic field through ω_{ci} , or the perpendicular pressure component P_{\perp} . The phase velocity increases with the κ index and parallel pressure P_{\parallel} and decreases with the positron temperature ratio σ . Moreover, it is found that the wave amplitude decreases with increasing ion pressure (P_{\parallel}) and the electron– positron temperature ratio (σ). On the contrary, the amplitude increases with rising superthermality κ , while collisions cause the wave amplitude to spread. The Coriolis force exclusively affects the width of electrostatic waves. The results of this study are particularly relevant for understanding wave behavior in astrophysical and space environments, especially within Earth's magnetosphere, where nonthermal electrons and positrons coexist with anisotropic pressure ions.

Keywords: anisotropic pressure, damped Zakharov–Kuznetsov equation, ion-acoustic waves, dissipative solitary waves, collisional plasma, kappa distribution, magnetized rotating plasma

1 Introduction

In recent years, the study of ion-acoustic waves (IAWs) in electron-positron-ion (e-p-i) plasma has garnered significant attention, enhancing our understanding of nonlinear phenomena in both space and laboratory settings [1–9]. IAWs are a pivotal feature of plasma systems, distinguished by their low-frequency oscillations primarily driven by ion motion and often accompanied by electron and positron density fluctuations. Washimi and Taniuti pioneered the investigation of ion-acoustic solitary waves (IASWs) in plasma [10], along with Sagdeev's theoretical framework [11]. This established a core nonlinear theory of IAWs, which Ikezi et al. [12] later validated through experiments. Since then, advancements in understanding IASWs have been noteworthy by many authors [13,14]. For instance, research on the dynamics of these waves in magnetized plasma has revealed both subsonic and supersonic compressive solitons, using the pseudopotential method to explore how various plasma parameters influence wave profiles [15]. Plasma waves have also been investigated in semiconductor materials during photothermal excitation

e-mail: samireltantawy@yahoo.com, tantawy@sci.psu.edu.eg Wedad Albalawi: Department of Mathematical Sciences, College of Science, Princess Nourah bint Abdulrahman University, P.O. Box 84428, Riyadh 11671, Saudi Arabia

Carlos A. Fotsing, Alim: Higher Teacher's Training College, University of Maroua, P.O. Box 55, Maroua, Cameroon

Alidou Mohamadou: National Advanced School of Engineering, University of Maroua, P.O. Box 46, Maroua, Cameroon

Rania A. Alharbey: Mathematics Department, Faculty of Science, King Abdulaziz University, Jeddah, Saudi Arabia

^{*} Corresponding author: Camus G. L. Tiofack, Faculty of Sciences, University of Maroua, P.O. Box 814, Maroua, Cameroon, e-mail: glatchio@yahoo.fr

^{*} Corresponding author: Samir A. El-Tantawy, Department of Physics, Faculty of Science, Al-Baha University, Al-Baha P.O. Box 1988, Saudi Arabia; Department of Physics, Faculty of Science, Al-Baha University, Port Said University, Port Said 42521, Egypt,

[16,17]. Studies on large-amplitude solitary waves in warm magnetoplasma have utilized the Sagdeev pseudopotential approach to examine wave structures across different amplitudes. Researchers have analyzed the impact of magnetic fields and plasma temperatures on the formation and stability of these waves, showing how factors like ion temperature and Mach number influence soliton behavior [18]. Additionally, investigations into small-amplitude solitary waves in magnetized ion-beam plasma have highlighted the coexistence of slow and fast modes under varying conditions [19]. Furthermore, recent studies have delved into the complex behaviors of nonlinear IAW structures such as periodic waves, solitary waves, and breathers in auroral magnetoplasmas [20].

The presence of a strong magnetic field in a collisionless medium results in plasma anisotropy, where the plasma exhibits distinct behaviors in parallel and perpendicular directions relative to the magnetic field [21]. The Chew-Goldberger-Low (CGL) theory [22], formulated in 1956, aptly describes this anisotropy, provided there is no coupling between the parallel and perpendicular degrees of freedom [23]. To analyze such plasmas, separate equations of state are required for the perpendicular and parallel ion pressures, denoted as $P_{i\perp}$ and $P_{i\parallel}$, where $P_{i\perp}(P_{i\parallel})$ are the perpendicular (parallel, respectively) components of the ion pressure relative to the ambient magnetic field. Wave-particle interactions may reduce this anisotropy by establishing correlations between these directions [24,25]. In space plasmas, phenomena such as plasma convection cause magnetic compression and expansion along field lines, leading to variations in the perpendicular and parallel temperatures [24]. These anisotropic conditions are commonly observed in regions like the magnetosphere and the near-Earth magnetosheath [21,26,27]. Adnan et al. investigated small amplitude ion-acoustic solitons in weakly magnetized plasma, focusing on anisotropic ion pressure [28]. Similarly, Chatterjee et al. examined obliquely propagating IASWs and double layers in magnetized dusty plasma with anisotropic ion pressure [29]. Additionally, the effects of pressure anisotropy on nonlinear electrostatic excitations in magnetized e-p-i plasmas were explored, revealing that anisotropic ion pressure significantly impacts the width and amplitude of solitary waves [30,31]. Furthermore, it was found that the increase in wave frequency induced by anisotropic ion pressure alters wave dispersion and enhances wave crest accumulation, potentially leading to the development of modified instability modes [32]. A decrease in pressure anisotropy has also been shown to enhance both the amplitude and width of dust-acoustic rogue waves [33,34]. Alternatively, the effect of a magnetic field on the motion of two rigid objects traveling linearly through an incompressible fluid with a couple stress characteristics has been explored [35].

The velocity distribution of plasma particles influences the behavior of wave motions in plasma. The Maxwellian distribution has been the standard choice for representing these particles for many decades. However, due to advancements in the study of space [36-39] and laboratory plasmas [40,41], non-Maxwellian particle distributions have become more prevalent. These distributions more accurately depict energetic particles with high-energy (superthermal) velocity distributions, often exhibiting superthermal tails. The Kappa velocity distribution is particularly effective in describing these tails. In 1968, Vasyliunas [36] introduced the Kappa distribution to match observational data. Today, this distribution is widely used to explain various astrophysical and space plasma phenomena, including those in the auroral zone [42], Earth's magnetosphere [43], in the interstellar medium [44], and in the solar wind [45]. Recent research has delved into the impact of superthermal electron distributions on solitary waves [46-49]. Saini et al. [50] examined the dynamics of electrostatic solitary excitations with superthermal electrons using a pseudopotential approach, concluding that for a fixed Mach number, the solitary wave profile becomes steeper and wider compared to typical plasma structures. Further studies on superthermal particles' role in electrostatic wave packets in electron-ion [51] and e-p-i [52,53] plasmas have shown, using the nonlinear Schrödinger equation, that superthermality increases the modulational instability of these wave packets. Singh et al. [54] recently studied the thermal effects of ions on IAWs in magnetized superthermal plasma via the Sagdeev potential approach, achieving results consistent with Viking satellite observations in the auroral region.

Wave propagation in plasmas with anisotropic pressure can experience significant changes. When introduced, magnetic fields induce the Lorentz force, which affects the motion of charged particles and modifies wave dispersion, stability, and energy redistribution [55]. Additionally, plasma rotation brings in the Coriolis force [56], which alters wave characteristics, especially in rotating plasma environments like fusion reactors or planetary magnetospheres [57]. These combined effects create a complex environment for understanding wave behavior. Theoretical and experimental studies have shown that even a weak Coriolis force can lead to interesting phenomena in astrophysical environments [57]. Given the Coriolis force's important role in rotating space plasmas, many researchers have attempted to analyze wave dynamics in the presence of the Coriolis force [58-61].

In addition to the effects of anisotropy and non-Maxwellian distributions, ion-neutral collisions play a crucial role in many plasmas. These collisions introduce dissipation and damping mechanisms that influence wave stability and soliton formation, acting as a source of energy loss and further complicating plasma dynamics. The behavior of IASWs in such complex plasmas can be described using extended nonlinear equations, such as the Zakharov-Kuznetsov (ZK) equation with a damping term. This equation incorporates the effects of anisotropy, magnetic fields, collisions, rotation, and non-Maxwellian velocity distributions. The ZK equation generalizes the Korteweg-de Vries equation to higher dimensions and can describe the evolution of ionacoustic solitons under various physical conditions. Several researchers have recently focused on studying dissipation phenomena in plasmas [62-64]. Their findings indicate that dissipation significantly impacts the profile of IASWs in plasma. While there has been extensive research on the effects of anisotropic ion pressure, studies on collisional magnetized nonthermal e-p-i rotating plasmas with superthermal electrons and positrons remain limited. This project aims to explore the nonlinear dynamics of ion-acoustic solitons in such a plasma, characterized by anisotropic, magnetized, and rotating conditions with a Kappa velocity distribution. The focus will be on understanding the influences of Coriolis forces, magnetic fields, ion-neutral collisions, and anisotropic pressure on soliton formation, stability, and propagation. By deriving and solving the ZK equation under these complex conditions, this study will deepen our comprehension of IAW dynamics in plasma systems with more realistic physical characteristics. These insights are essential for advancing our knowledge of phenomena in space physics, fusion research, and astrophysical systems.

This article is organized as follows: The basic governing equations for describing our anisotropy e-p-i plasma system are shown in Section 2. In Section 3 linear structure is carried out. Section 4 contains the derivation of the damped Zakharov-Kuznetsov (dZK)-type equation using the reductive perturbation method (RPM). The analytical solutions representing dissipated solitary pulses are given in Section 4.1 and numerical simulations are shown in Section 4.2. Finally, the summary of our research work is concluded in Section 5.

2 Basic governing equations

We consider a collisional, magnetized, three-component e-p-i plasma that rotates under the influence of the Coriolis force. The electrons and positrons in this plasma

are superthermal, while the ions experience weak collisions with neutrals. These ions are considered inertial $(m_i \gg m_{e,p})$, having mass m_i , velocity u_i , charge $Z_i e$, collision frequency v_n , and an anisotropic ion pressure tensor \bar{P}_i modeled by the CGL theory [22]. The magnetic field is uniform and oriented along the \vec{z} -axis $(\vec{B} = B_0 \vec{e}_z)$. The plasma rotates with a low frequency Ω_0 around the \vec{z} -axis due to the Coriolis effect, with negligible centrifugal force. We assume that the electrostatic wave propagates in all three spatial directions, i.e., $\vec{\nabla} = (\partial_x, \partial_y, \partial_z)$. At thermal equilibrium, the plasma composition is such that $\mu_e = 1 + \mu_n$, where $\mu_s = n_{s0}/n_{i0}$, with n_{i0} and $n_{s0}(s = e, p)$ denoting the equilibrium number densities of ions, electrons, and positrons, respectively. The following basic equations govern the dynamics of IAWs in the current plasma model [28,30,62]:

$$\partial_t n_i + \nabla \cdot (n_i \mathbf{u}_i) = 0, \tag{1}$$

$$\partial_{t} \boldsymbol{u}_{i} + (\boldsymbol{u}_{i} \cdot \nabla) \boldsymbol{u}_{i} + \frac{Z_{i} \boldsymbol{e}}{m_{i}} \nabla \phi - \frac{Z_{i} \boldsymbol{e}}{m_{i} c} B_{0} \boldsymbol{u}_{i} \wedge \boldsymbol{e}_{z}$$

$$- 2\boldsymbol{u}_{i} \wedge \Omega + \frac{1}{m_{i} n_{i}} \nabla \cdot \bar{\boldsymbol{p}}_{i} + \nu_{n} \boldsymbol{u}_{i} = 0,$$
(2)

$$\nabla^2 \phi = -4\pi e (n_p + Z_i n_i - n_e), \tag{3}$$

where e denotes the elementary charge, n_s denotes the number density of particle s(s = e, p, i), and ϕ denotes the electrostatic potential. \bar{P}_i represents the pressure tensor. The number densities of electrons and positrons are defined by [28]

$$n_s = n_{s0} \left[1 + \frac{q_s \phi}{k_B T_s (\kappa_s - 3/2)} \right]^{-(\kappa_s - 1/2)},$$
 (4)

with $q_s = e$ if s = p and $q_s = -e$ if s = e.

In this work, the pressure differs between the perpendicular and parallel directions, leading to plasma anisotropy under a strong magnetic field. Consequently, the pressure tensor takes the form [65]

$$\bar{\bar{\boldsymbol{p}}}_{i} = \begin{pmatrix} P_{i\perp} & 0 & 0 \\ 0 & P_{i\perp} & 0 \\ 0 & 0 & P_{i\parallel} \end{pmatrix} = P_{i\perp}\bar{\bar{\boldsymbol{I}}} + (P_{i\parallel} - P_{i\perp})\boldsymbol{e}_{z}\boldsymbol{e}_{z},$$
 (5)

where $ar{m{I}}$ is the unit tensor and $m{e}_{\!\scriptscriptstyle Z}$ is the unit vector along the magnetic field direction. According to the CGL theory [22], the scalar pressures $P_{i\perp}$ and $P_{i\parallel}$ are defined as follows:

$$P_{i\perp} = P_{i0\perp} \frac{n_i}{n_{i0}}; \ P_{i\parallel} = P_{i0\parallel} \left(\frac{n_i}{n_{i0}}\right)^3,$$
 (6)

where $P_{i0\perp}(Z_in_{i0}k_BT_{i\perp})$ and $P_{i0\parallel}(Z_in_{i0}k_BT_{i\parallel})$ define the perpendicular and parallel pressures, respectively, at equilibrium. In isotropic plasmas, $P_{i\perp} = P_{i\parallel}$. In the three spatial

directions (x, y, z) through which the wave propagates, the plasma dynamics equations are as follows:

$$\partial_t n_i + \partial_x (n_i u_{ix}) + \partial_y (n_i u_{iy}) + \partial_z (n_i u_{iz}) = 0, \tag{7}$$

$$n_i \partial_t u_x + n_i (u_x \partial_x + u_y \partial_y + u_z \partial_z) u_x + n_i \partial_x \Phi$$

$$- (\omega_{ci} + 2\Omega_0) n_i u_y + P_{i-1} \partial_x n_i + \nu_n n_i u_x = 0,$$
(8)

$$n_i \partial_t u_y + n_i (u_x \partial_x + u_y \partial_y + u_z \partial_z) u_y + n_i \partial_y \Phi + (\omega_{ci} + 2\Omega_0) n_i u_x + P_{i+} \partial_y n_i + \nu_n n_i u_y = 0,$$
(9)

$$\partial_t u_z + (u_x \partial_x + u_y \partial_y + u_z \partial_z) u_z + \partial_z \Phi + P_{i||n_i} \partial_z n_i + v_n u_z = 0,$$
(10)

$$(\partial_x^2 + \partial_y^2 + \partial_z^2)\Phi + n_i - 1 - \alpha_1\Phi - \alpha_2\Phi^2 - \alpha_3\Phi^3 + \dots = 0,$$
(11)

where the coefficients α_1 , α_2 , and α_3 are functions of the κ parameter given by

$$\alpha_{1} = (1 + (1 + \sigma)\mu_{p}) \frac{(\kappa - 1/2)}{(\kappa - 3/2)},$$

$$\alpha_{2} = (1 + (1 - \sigma^{2})\mu_{p}) \frac{(\kappa^{2} - 1/4)}{2(\kappa - 3/2)^{2}},$$

$$\alpha_{3} = (1 + (1 + \sigma^{3})\mu_{p}) \frac{(\kappa^{2} - 1/4)(\kappa + 3/2)}{6(\kappa - 3/2)^{3}},$$
(12)

with $\kappa_e = \kappa_p = \kappa$ for simplification of calculations.

Here, n_i is the ion number density normalized by its equilibrium value n_{i0} , u is the ion velocity considered fluid and normalized by the ion sound speed $C_{si}(=(Z_ik_BT_e/m_i)^{1/2})$, and Φ is the electrostatic potential normalized by k_BT_e/e . The time variable is normalized by the plasma frequency $\omega_{pi}(=(4\pi Z_in_{i0}e^2/m_i)^{1/2})$. The spatial variables x,y, and z are normalized by the Debye length $\lambda_{Di}(=(k_BT_e/4\pi Z_in_{i0}e^2)^{1/2})$. Here, k_B is the Boltzmann constant, e is the elementary charge, and $\sigma(=T_e/T_p)$ is the temperature ratio of electrons to positrons.

3 Linear structure

The analysis involves performing a Fourier analysis of Eqs. (7)–(11), assuming small perturbations of the form $\sim \exp[j(\vec{k}\cdot\vec{r}-\omega t)]$ around the equilibrium value, where $j^2=-1, k^2=k_\perp^2+k_\parallel^2$, with $k_\perp^2=k_x^2+k_y^2$ and $k_\parallel^2=k_z^2$, and ω represents the perturbation frequency. In the limit of large wavelength values $(k\ll 1)$, the dispersion relation of waves propagating in a uniform magnetic field with anisotropic ion pressure is obtained and defined as

$$-\omega + \left(\frac{1}{k^{2} + \alpha_{1}} + P_{\perp}\right) \frac{(\omega + j\nu)k_{\perp}^{2}}{(\omega + j\nu)^{2} - (\omega_{ci} + 2\Omega_{0})^{2}} + \left(\frac{1}{k^{2} + \alpha_{1}} + P_{\parallel}\right) \frac{k_{\parallel}^{2}}{(\omega + j\nu)} = 0,$$
(13)

where $\nu = \nu_n$. In the case of a non-collisional plasma ($\nu = 0$) and low rotation ($\omega_{ci} \gg \Omega_0$), the dispersion relation reduces to

$$\left(\frac{1}{k^2 + \alpha_1} + P_{\perp}\right) \frac{k_{\perp}^2}{\omega^2 - \omega_{ci}^2} + \left(\frac{1}{k^2 + \alpha_1} + P_{\parallel}\right) \frac{k_{\parallel}^2}{\omega^2} = 1. \quad (14)$$

Eq. (14) defines the dispersion relation of waves in a non-collisional and non-rotational magnetized e–p–i plasma with anisotropic ion pressure. In this limiting case, Eq. (14) aligns with Eq. (21) in Adnan et~al. [30] and Eq. (32) in Ullah Khan et~al. [66]. Solving Eq. (14) reveals two ion oscillation modes within this model: the slow or acoustic mode, characterized by the frequency ω_- , and the fast mode, characterized by the frequency ω_+ such that

$$\omega_{\pm}^2 = \frac{1}{2}F \pm \frac{1}{2}\sqrt{F^2 - 4C},\tag{15}$$

where
$$F = \left(\frac{k^2}{k^2 + \alpha_1} + P_{\perp}k_{\perp}^2 + P_{||}k_{||}^2 + \omega_{ci}^2\right)$$
 and $C = \left(\frac{1}{k^2 + \alpha_1} + P_{||}\right)k_{||}^2\omega_{ci}^2$.

Next, we will examine the behavior of ion oscillations in both the perpendicular and parallel directions of the magnetic field.

3.1 Parallel component

To consider the propagation of the wave in the direction of the magnetic field, we set k_{\perp} = 0 and k_{\parallel} = k. Consequently, Eq. (13) becomes

$$\omega^2 + jv\omega - \left(\frac{1}{k^2 + a_1} + P_{||}\right)k^2 = 0.$$
 (16)

The solution to this equation is complex and expressed as $\omega = \omega_r + j\omega_{im}$, given by

$$\omega_r = \pm \left[\left(\frac{1}{k^2 + \alpha_1} + P_{||} \right) k^2 - \frac{1}{4} v^2 \right]^{1/2},$$

$$\omega_{im} = -\frac{1}{4} v^2.$$
(17)

Ion damping occurs due to collisions between ions and neutrals. For large wavelengths ($k \ll 1$), there is a threshold value k_s for the wavenumber below which the wave is damped. Consequently, ion oscillations occur in the

medium when $k_s < k \ (\omega_r^2 > 0)$. In this context, k_s is defined as

$$k_s = \frac{v}{2} \sqrt{\frac{\alpha_1}{1 + \alpha_1 P_{||}}}.$$
 (18)

For $k_s > k$, ion oscillations cease, and the medium becomes strongly dissipative.

We will now numerically analyze the behavior of the dispersion relation in Eq. (16) for various values of the spectral parameter (κ) , the positron concentration (μ_p) , the pressure (P_{\parallel}) , the temperature ratio (σ) , and the collision frequency (ν) .

Figure 1 depicts the linear properties of the dispersion concerning the wavenumber k. Figure 1(a) demonstrates that the frequency of ion oscillations increases with both the wavenumber k and the spectral parameter. The superthermality of the plasma induces ion instability at low

wavenumbers. The spectral index κ does not affect the imaginary part of the wave frequency.

Figure 1(b) illustrated the variations of the real part of the oscillation frequency ω_r as a function of the wavenumber k, for different values of the anisotropic pressure (P_{\parallel}) . The oscillation frequency increases with both the wavenumber k and the anisotropic pressure (P_{\parallel}) . The pressure anisotropy does not affect the oscillation frequency for large wavelengths, where the oscillation frequency remains nearly constant. For short wavelengths, the pressure anisotropy increases the oscillation frequency. The pressure anisotropy does not impact the imaginary part of the oscillations ω_{im} . Figure 2 illustrates the parameter σ and positron concentration μ_n effects on the ion frequency ω_r . It shows that the ion frequency decreases with increasing temperature ratio σ (panel (a)) and increasing positron concentration μ_n (panel (b)), while it increases with the wavenumber k. Like the spectral

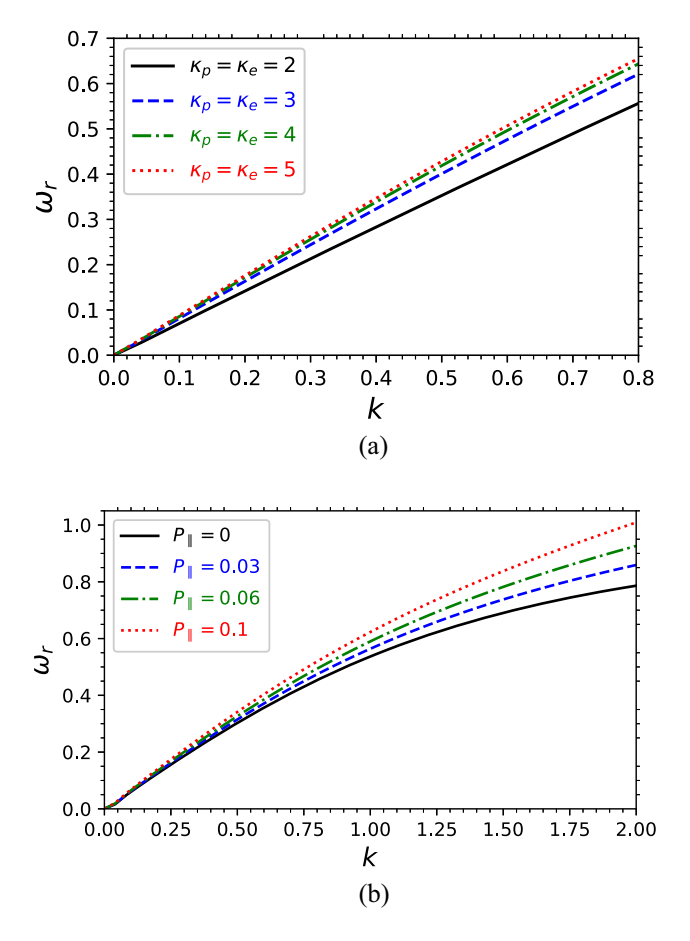
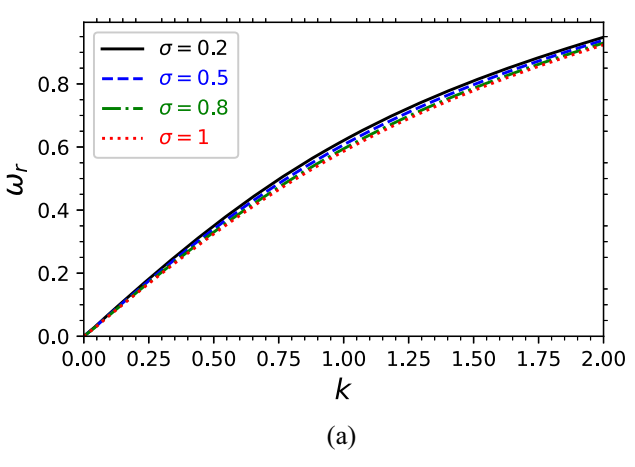


Figure 1: Plot of the real part of wave frequency ω_r versus wavenumber k (a) for different values of the spectral parameter κ with $\mu_p=0.4$, $\sigma=0.5$, $P_{||}=0.3$, and $\nu=0.02$ and (b) for different values of parallel component of anisotropy pressure $P_{||}$ with $\mu_p=0.4$, $\kappa=3$, $\sigma=0.2$, and $\nu=0.04$.



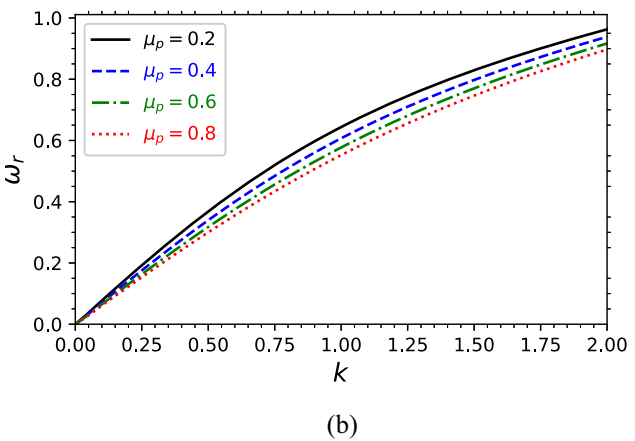


Figure 2: Plot of the real part of wave frequency ω_r : (a) for different values of ratio temperature σ with $\mu_p=0.5$ and (b) for different values of concentration of positron μ_p with $\sigma=0.5$ where $\kappa=4$, $P_{\parallel}=0.06$, and $\nu=0.02$.

parameter κ and anisotropic pressure (P_{\parallel}) , σ and μ_p have no effects on the imaginary frequency ω_{im} .

Figure 3 demonstrates that the imaginary part of the oscillation frequency is negative and consists of two regimes: the transient regime $(0 \le k \le 0.04)$ and the permanent regime $(k \ge 0.04)$. The transient regime corresponds to the decreasing variations of the imaginary frequency (ω_{im}) . This is because for some values of the wavenumber below the threshold wavenumber k_s (Eq. (17)), the real part of the frequency becomes imaginary. This transient regime results from damping oscillations, i.e., the wavenumber is below the threshold wavenumber $(k < k_s)$. The threshold wavenumber is $k_s = 0.04$. The permanent regime $(k \ge 0.04)$ is constant and corresponds to $\omega_{im} = -\nu/2$. An increase in collision frequency leads to strong attenuation of oscillations in the plasma.

We have demonstrated that the parallel component P_{\parallel} of the anisotropic pressure increases the ion oscillation frequency without affecting the damping of these oscillations. Now, let us consider the influence of the perpendicular component P_{\perp} on ion oscillations.

3.2 Perpendicular component

In the direction perpendicular to the uniform magnetic field, we assume the wavenumber in the parallel direction to be zero $(k_{\parallel} = 0)$ and the wavenumber in the perpendicular direction to be $k_{\perp} = k$. Thus, Eq. (13) reduces to:

$$\omega^{3} + 2jv\omega^{2} - \left[\left(\frac{1}{k^{2} + \alpha_{1}} + P_{\perp} \right) k^{2} + (\omega_{ci} + 2\Omega_{0})^{2} + v^{2} \right] \omega$$

$$- j \left(\frac{1}{k^{2} + \alpha_{1}} + P_{\perp} \right) v k^{2} = 0.$$
(19)

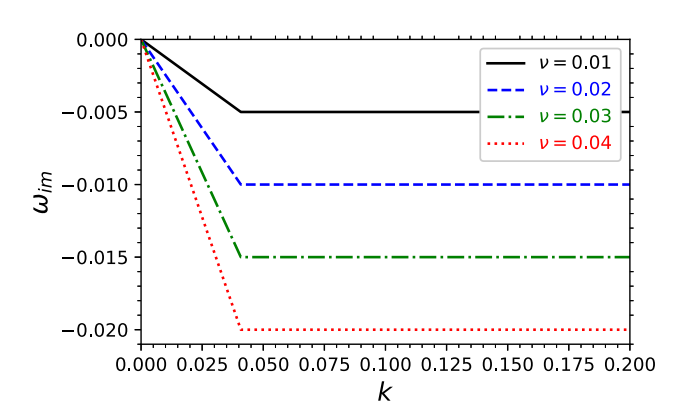


Figure 3: Plot of the imaginary part of frequency versus wavenumber k for different values of collision frequency ν with parameters fixed: $\mu_p = 0.4$, $\kappa = 5$, $\sigma = 0.5$, and $P_{\parallel} = 0.05$.

The complex solutions $(\omega_r; \omega_{im})$ of this Eq. (19) are obtained by the Cardan method and are given by

$$\omega_{r} = \frac{\sqrt{3}}{2}(r + r'),$$

$$\omega_{im} = \frac{1}{2}(r - r') - \frac{b_{0}}{3},$$
(20)

where

$$r = \sqrt[3]{\frac{1}{2} \left(q_0 + \sqrt{q_0^2 + \frac{4}{27} p_0^3} \right)},$$

$$r' = \sqrt[3]{\frac{1}{2} \left(-q_0 + \sqrt{q_0^2 + \frac{4}{27} p_0^3} \right)},$$

$$q_0 = \frac{1}{27} (-2b_0^3 + 9c_0b_0 - 27d_0),$$

$$p_0 = \frac{1}{3} (3c_0 - b_0^2),$$

$$d_0 = \left(\frac{1}{k^2 + a_1} + P_\perp \right) v k^2,$$

$$c_0 = \left(\frac{1}{k^2 + a_1} + P_\perp \right) k^2 + (\omega_{ci} + 2\Omega_0)^2 + v^2,$$

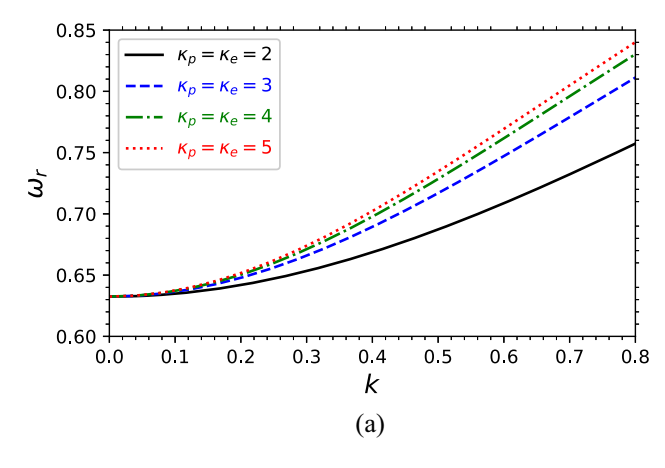
$$b_0 = 2v.$$
(21)

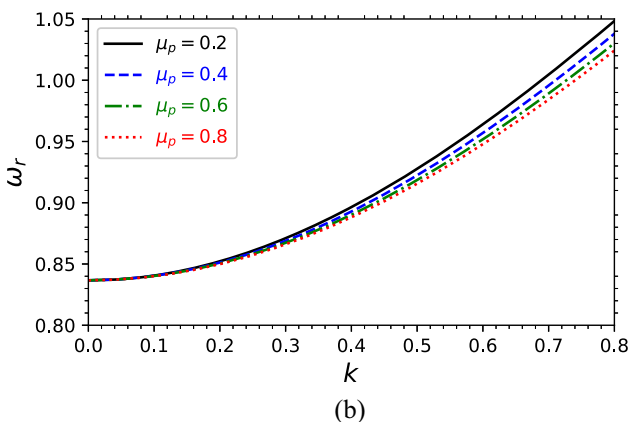
Assuming no collisions $(\nu \to 0)$, low plasma rotation $(\omega_{ci} \gg \Omega_0)$, and cold ions $(P_{\perp} = 0)$ in a Maxwellian plasma with $n_{eo} = n_{p0}$ and $T_e = T_p$, Eq. (19) becomes

$$\omega^2 - \left(\omega_{ci}^2 + \frac{k^2}{k^2 + (1+\sigma)\mu_p}\right) = 0.$$
 (22)

This Eq. (22) is similar to Eqs. (30) and (21) in previous studies [62,67], respectively. The difference lies in the normalization condition and the distribution function used.

The numerical study of the dispersion relation in the direction perpendicular to the magnetic field is presented in the following paragraph. As with the parallel component, we will investigate the impact of plasma parameters $(\kappa, \mu_n, \sigma, \Omega_0, P_\perp, \nu)$ on ion oscillations. Figure 4 shows the variation of the frequency as a function of the wavenumber k. Figure 4(a) illustrates the variation of the real part of the frequency as a function of the wavenumber k for different values of the spectral parameter κ . The oscillation frequency increases with the wavenumber k. An increase in the spectral parameter leads to a rise in the oscillation frequency. For zero wavenumber, the frequency is non-zero (ω = 0.63), indicating the existence of electrostatic waves. Figure 4(b) indicates that an increase in positron concentration leads to a decrease in ion frequency, resulting in greater stability for these ions. Conversely, the frequency increases with the wavenumber k. Higher wavenumbers correspond to higher frequencies of





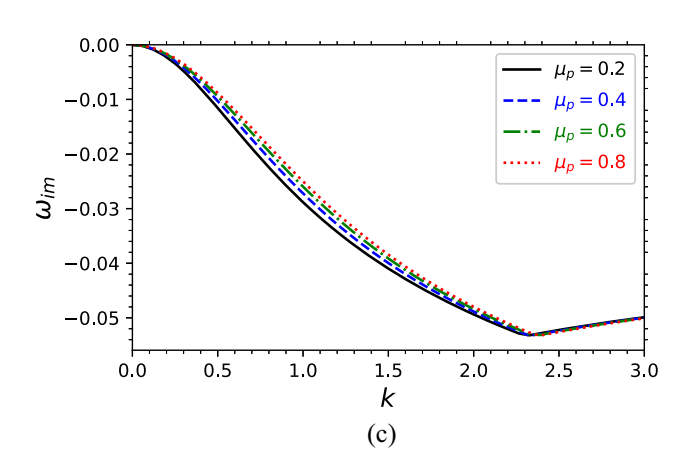


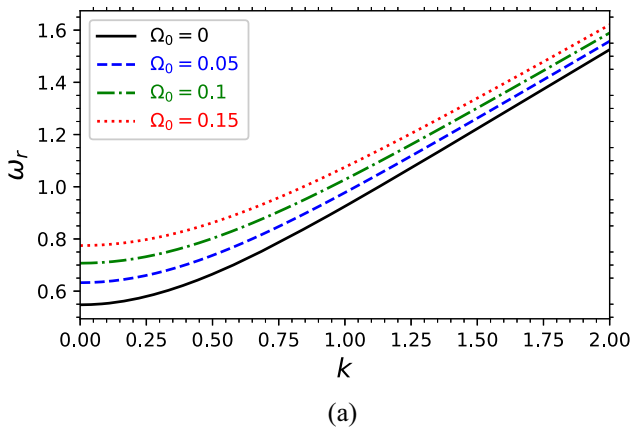
Figure 4: The variation of wave frequency versus wavenumber k. (a) Real part frequency ω_r for different values of the spectral parameter κ with $\mu_p=0.2,\,\sigma=0.8,\,P_\perp=0.06,\,\Omega_0=0.05,\,\omega_{ci}=0.3$ and $\nu=0.03$. (b) Real part frequency ω_r for different values of concentration positron μ_p and (c) imaginary part for different values of concentration positrons μ_p with $\sigma=0.5,\,\kappa=4,\,P_\perp=0.4,\,\Omega_0=0.6,\,\omega_{ci}=0.3,\,$ and $\nu=0.08$.

ion oscillations. The positron concentration raises the frequency of electrostatic waves ($\omega \approx 0.84$; $k \to 0$) compared to the influence of the spectral parameter ($\omega = 0.63$; $k \to 0$). Figure 4(c) illustrates the decrease in the imaginary part of the ion frequency with the

wavenumber k. We observe that an increase in positrons leads to a reduction in the damping of oscillations in the transient regime k < 2.3, thereby diminishing the effect of energy dissipation in the plasma.

For k > 2.3, the frequency ω_{im} becomes constant (permanent regime). The frequency ω_{im} remains negative, indicating the damping of ion oscillations in this plasma model. Just as with positron concentration, a decrease in positron temperature (σ) reduces the oscillation frequency ω_r . Notably, the frequency ω_r increases when k=0 ($\omega_r \approx 1.22$ when k=0) compared to the parameters μ_p and κ (curve not shown).

In Figure 5, we investigate the effects of plasma rotation on the real and imaginary components of the dispersion relation. Figure 5(a) shows that the frequency of electrostatic wave oscillations and the wavenumber k increase with an increase in the plasma rotation frequency. For infinite wavenumbers, the oscillation frequency becomes linear and is no longer affected by plasma



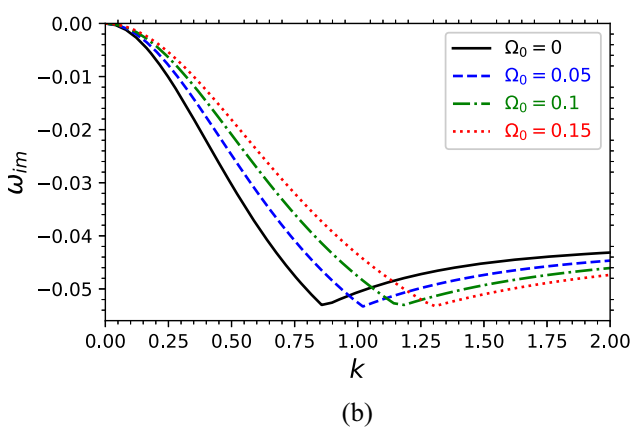


Figure 5: The variation of wave frequency versus wavenumber k. (a) Real part frequency ω_r and (b) imaginary part for different values of plasma rotating frequency Ω_0 with parameters fixed σ = 0.5, κ = 4, P_\perp = 0.4, μ_p = 0.6, ω_{ci} = 0.3 and ν = 0.08.

rotation. Therefore, the plasma rotation frequency does not influence wave oscillations at short wavelengths. Figure 5(b) shows that the imaginary part of the frequency is always negative due to the effects of oscillation damping. The frequency ω_{im} decreases as a function of the wavenumber k and passes through a critical value k_c (which varies depending on the values of Ω_0), then changes concavity and becomes constant beyond a particular value of k. Additionally, as the plasma rotation frequency increases, the frequency ω_{im} decreases, indicating that the oscillations become less damped. The permanent regime is characterized by the wavenumber values where the frequency ω_{im} remains constant and negative.

The collision frequency does not affect the real part of the frequency (curve not shown). The variation of the imaginary part of the wave frequency as a function of k is always negative. It presents two zones: a decreasing part (transient zone) and a part where the frequency remains constant (permanent regime), as shown in Figure 6. However, the collision frequency strongly affects the imaginary component ω_{im} . The higher the collision frequency, the more ω_{im} decreases, making the wave oscillations more damped.

In Figure 7, we have plotted the real and imaginary components of ω as a function of the wavenumber k for four different values of the perpendicular component of the anisotropy pressure. Figure 7(a) shows that for short wavelengths, the growth rate of the ion acoustic frequency ω_r increases with the wavenumber k and with increasing values of the anisotropy pressure P_{\perp} . The increase in ion pressure P_{\perp} leads to instability of IAWs. Pressure anisotropy does not affect waves at low wave numbers, ensuring stability. It should be noted that in the absence of anisotropy pressure $(P_{\perp}=0)$, the frequency of ion waves tends to a constant limit value. Figure 7(b) shows that ω_{im} decreases as a function of k up to a critical value of the

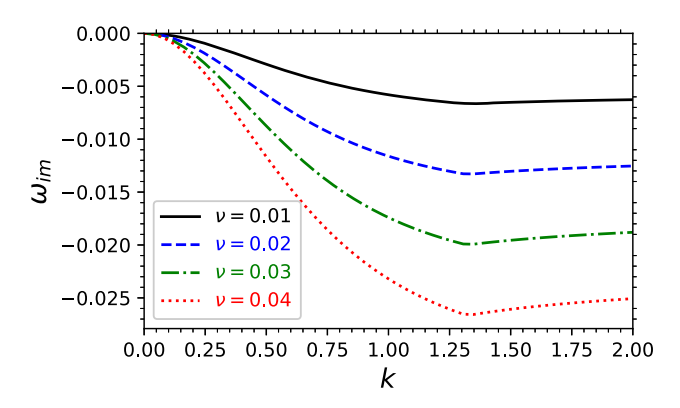
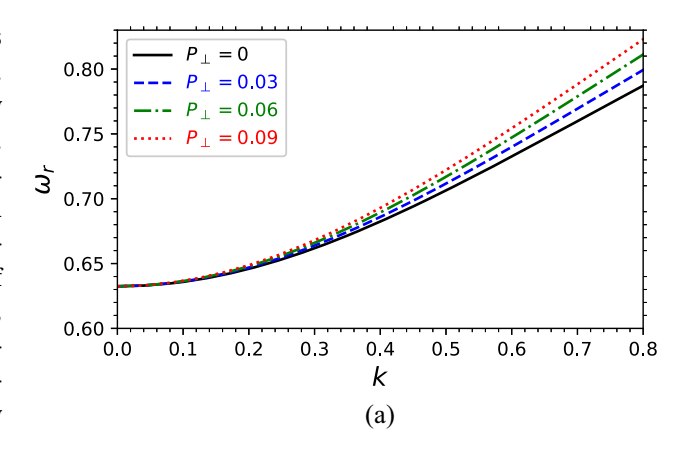


Figure 6: Plot of the imaginary part of the frequency as a function of k for different values of ν with σ = 0.8, κ = 2, P_{\perp} = 0.006, μ_p = 0.2, ω_{ci} = 0.3, and Ω_0 = 0.05.



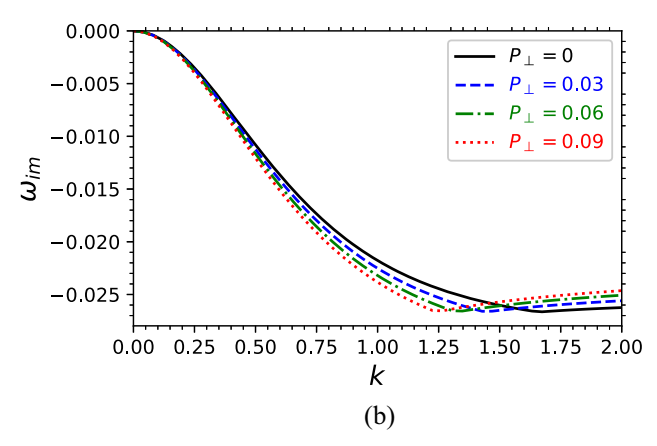


Figure 7: Variation of the real part ω_r (a) and the imaginary part ω_{im} (b) of the wave frequency against the wave number k for different values of P_{\perp} . Along with $\sigma=0.8$, $\kappa=2$, $\nu=0.04$, $\mu_p=0.2$, $\omega_{ci}=0.3$, and $\Omega_0=0.05$.

wavenumber $(k < k_c)$, then changes concavity $(k > k_c)$ and becomes constant at higher wavenumbers. For $k < k_c$, the increase in ion pressure anisotropy decreases the imaginary component of the frequency, causing the oscillations to become more damped. Conversely, for $k > k_c$, the anisotropy increases the frequency ω_{im} , reducing the damping effect.

4 Nonlinear structure

In this section, we transform Eqs (7)–(11) into a single nonlinear equation that encapsulates the dynamics of IASWs. This transformation will be accomplished through the RPM, which effectively examines the nonlinear properties of finite-amplitude waves. We can streamline the system's complexity by utilizing the concept of stretched coordinates. The independent variables are defined as follows:

$$X = \varepsilon^{1/2}x$$
, $Y = \varepsilon^{1/2}y$, $Z = \varepsilon^{1/2}(z - v_n t)$, $T = \varepsilon^{3/2}t$, (23)

with $0 < \varepsilon \ll 1$ as the parameter indicating the weakness of nonlinearity, and v_p representing the phase velocity of the wave. We will expand the perturbed quantities in terms of a power series in ε around their equilibrium values as follows:

$$n_{i} = 1 + \varepsilon n_{i}^{(1)} + \varepsilon^{2} n_{i}^{(2)} + \varepsilon^{3} n_{i}^{(3)} + \cdots ,$$

$$u_{x,y} = \varepsilon^{3/2} u_{x,y}^{(1)} + \varepsilon^{3} u_{x,y}^{(2)} + \varepsilon^{5/2} u_{x,y}^{(3)} + \cdots ,$$

$$u_{z} = \varepsilon u_{z}^{(1)} + \varepsilon^{2} u_{z}^{(2)} + \varepsilon^{3} u_{z}^{(3)} + \cdots ,$$

$$\Phi = \varepsilon \Phi^{(1)} + \varepsilon^{2} \Phi^{(2)} + \varepsilon^{3} \Phi^{(3)} + \cdots ,$$

$$v_{n} = \varepsilon^{3/2} v_{0}.$$
(24)

Considering Eqs (23) and (24) in Eqs (7)–(11), we derive at first order in ε

$$u_{x}^{(1)} = -\frac{1 + P_{\perp}\alpha_{1}}{\omega_{ci} + 2\Omega_{0}} \partial_{Y} \Phi^{(1)},$$

$$u_{y}^{(1)} = \frac{1 + P_{\perp}\alpha_{1}}{\omega_{ci} + 2\Omega_{0}} \partial_{X} \Phi^{(1)},$$

$$u_{z}^{(1)} = v_{p} n_{i}^{(1)} = \frac{1}{v_{p}} \Phi^{(1)} + \frac{P_{\parallel}}{v_{p}} n_{i}^{(1)},$$

$$n_{i}^{(1)} = \alpha_{1} \Phi^{(1)}.$$
(25)

By combining the components $u_z^{(1)}$ and $n_i^{(1)}$, we derive the phase velocity v_p of IAW propagation

$$v_p^2 = \frac{1}{\alpha_1} + P_{||}. (26)$$

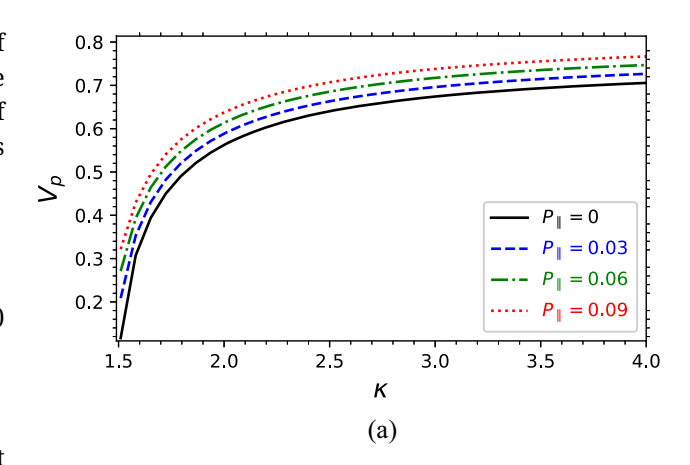
Notably, the phase velocity v_p is independent of the perpendicular pressure component P_\perp . Instead, this speed is influenced by the spectral parameter κ , the positron concentration μ_p through α_1 , and the parallel pressure component P_\parallel . The phase velocity v_p increases with both the parallel pressure component and the spectral index κ , as illustrated in Figure 8(a). Conversely, this speed decreases with increasing ratio temperature σ , as shown in Figure 8(b). It is also noteworthy that for $\kappa=3/2$, the phase velocity is not defined. As $\kappa\to\infty$, the phase velocity reaches a steady state, rendering the waves stable. Therefore, IAWs achieve stability exclusively in Maxwellian plasmas. Proceeding with the development to second order in $\varepsilon^{1/2}$, we obtain

$$u_{x}^{(2)} = v_{p} \frac{1 + P_{\perp} \alpha_{1}}{(\omega_{ci} + 2\Omega_{0})^{2}} \partial_{ZX}^{2} \Phi^{(1)},$$

$$u_{y}^{(2)} = v_{p} \frac{1 + P_{\perp} \alpha_{1}}{(\omega_{ci} + 2\Omega_{0})^{2}} \partial_{ZY}^{2} \Phi^{(1)},$$
(27)

as well as at second order in ε of the Poisson equation, we have

$$(\partial_X^2 + \partial_Y^2 + \partial_Z^2)\Phi^{(1)} + n_i^{(2)} - \alpha_1 \Phi^{(2)} - \alpha_2 \Phi^{(1)^2} = 0.$$
 (28)



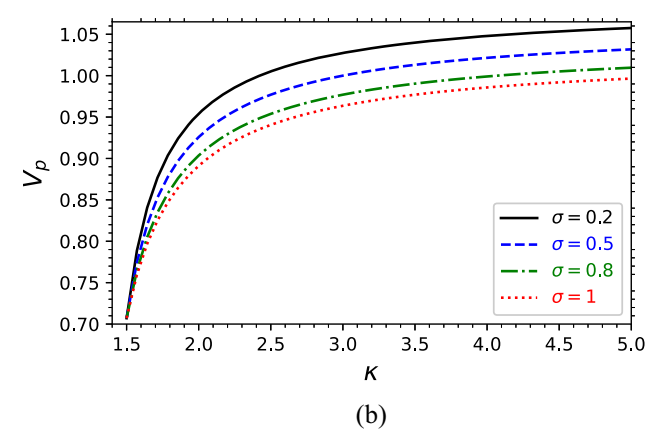


Figure 8: Plot phase speed v_p versus the superthermality index κ for different values: (a) of anisotropy pressure parallel component P_{\parallel} where σ = 0.8 and (b) of concentration positrons σ where P_{\parallel} = 0.5 with parameter fixed μ_p = 0.4.

At third order in the $\varepsilon^{1/2}$ expansion for the continuity equations and the z component of the momentum equation, incorporating Eqs (25)–(27) and combining them with the derivative with respect to Z of Eq. (28), we derive the following nonlinear differential equation:

$$\partial_T \Phi^{(1)} + A \Phi^{(1)} \partial_Z \Phi^{(1)} + B \partial_Z (\partial_X^2 + \partial_Y^2) \Phi^{(1)} + C \partial_Z^3 \Phi^{(1)} + \nu \Phi^{(1)} = 0.$$
(29)

with

$$A = C[\alpha_1^2(3 + 4\alpha_1 P_{||}) - 2\alpha_2],$$

$$B = C\left[1 + \frac{(1 + \alpha_1 P_{||})(1 + \alpha_1 P_{\perp})}{(\omega_{ci} + 2\Omega_0)^2}\right],$$

$$C = \frac{1}{2\sqrt{\alpha_1^3(1 + \alpha_1 P_{||})}},$$

$$v = \frac{v_0}{2}.$$
(30)

Eq. (29) is recognized as the dZK nonlinear equation, which incorporates the nonlinear coefficient *A*, dispersion

10

coefficients B, C, and dissipation ν , all defined in Eq. (30). Our results align with previous works regarding the limiting cases discussed. For example, in the absence of collisions ($\nu=0$) with neutrals, positrons $\mu_p=0$, and the Coriolis force $\Omega_0=0$, Eq. (30) matches Eq. (33) from the study of Adnan et~al. [28]. In the case of a non-collisional e–p–i plasma with low rotation ($\omega_{ci}\gg\Omega_0$) within a uniform magnetic field, where propagation takes place in the (y; z) plane, Eqs (29) and (30) are equivalent to equations (39) and (40) found in the study of Adnan et~al. [30].

4.1 Solitary pulse solution

To model the existence of electrostatic waves qualitatively, we typically consider a solitary wave solution of the dZK Eq. (29), analogous to the KdV equation. However, the dZK Eq. (29) is a non-integrable system due to collisions between ions and neutrals ($\partial_T E \neq 0$). We will simplify this by adopting an approximate solution of Eq. (29), neglecting collisions, and introducing the independent variable:

$$\zeta = l_x X + l_y Y + l_z Z - u_0 T, \tag{31}$$

where l_x , l_y , and l_z are the direction cosines of the wave vector \vec{k} such that $l_x^2 + l_y^2 + l_z^2 = 1$, u_0 the constant propagation velocity of the soliton. By neglecting collisions, we obtain the standard ZK equation given by [68]

$$\partial_T \Phi^{(1)} + A \Phi^{(1)} \partial_Z \Phi^{(1)} + B \partial_Z (\partial_X^2 + \partial_Y^2) \Phi^{(1)} + C \partial_Z^3 \Phi^{(1)}$$
= 0

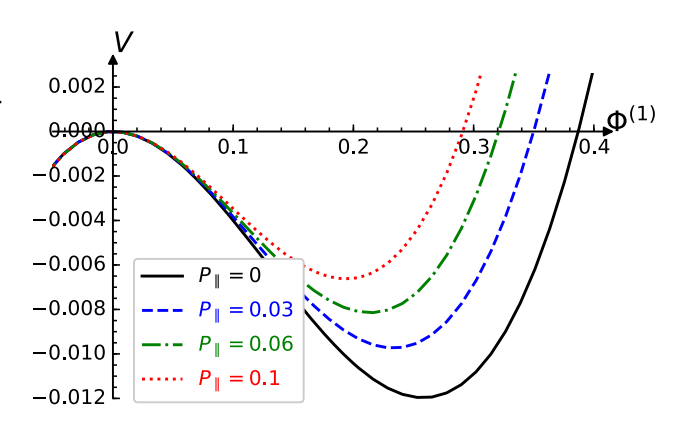
By introducing the variable defined in (31) into Eq. (32), we obtain the following energy density:

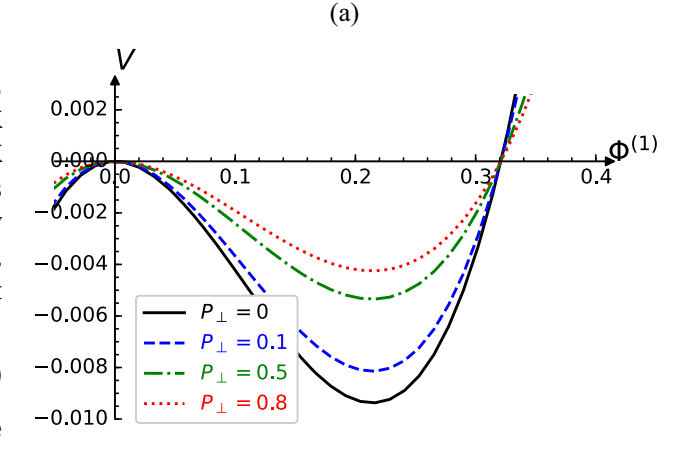
$$\frac{1}{2} \left[\frac{\mathrm{d}\Phi^{(1)}}{\mathrm{d}\zeta} \right]^2 + V(\Phi^{(1)}) = 0, \tag{33}$$

where $V(\Phi^{(1)})$ is the pseudo-potential defined by

$$V(\Phi^{(1)}) = -\frac{1}{2} \frac{u_0}{l_z [l_z^2 C + B(l_x^2 + l_y^2)]} \times \Phi^{(1)^2} \left[1 - \frac{A}{3u_0} \Phi^{(1)} \right].$$
(34)

Figure 9 shows the impact of P_{\perp} , P_{\parallel} , and Ω_0 on the pseudopotential V. This potential exhibits a compressive solitary wave structure with a single well. It is shown that as P_{\parallel} and P_{\perp} grow, the potential depth decreases (Figure 9(a) and (b)), leading to a reduction in both the amplitude and width of the compressive solitary waves. In contrast, Figure 9(c) demonstrate the opposite behavior where it is observed that the amplitude and width of the corresponding





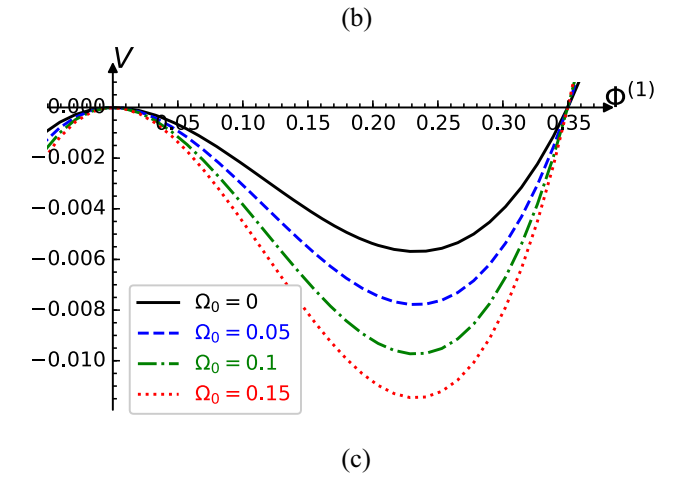


Figure 9: Variation of pseudo-potential V against $\Phi^{(1)}$ for different values of parallel pressure component P_{\parallel} (a) with $\Omega_0=0.1$ and $P_{\perp}=0.1$, perpendicular pressure component P_{\perp} (b) with $\Omega_0=0.1$ and $P_{\parallel}=0.06$, Coriolis force parameter (c) with $P_{\perp}=0.1$ and $P_{\parallel}=0.03$. Parameters fixed: $\kappa=3$, $\mu_p=0.6$, $\sigma=0.2$, and $\omega_{ci}=0.4$.

compressive soliton become greater as Ω_0 enhances. The integration of Eq. (33) provides the soliton solution described by

$$\Phi^{(1)}(\zeta) = \Phi_0^{(1)} \operatorname{sech}^2(\zeta/L),$$
 (35)

where $\Phi_0^{(1)}$ denotes the amplitude and L represents the width of the soliton, defined by

$$\Phi_0^{(1)} = \frac{3u_0}{Al_z},$$

$$L = \sqrt{\frac{4l_z[Cl_z^2 + B(l_x^2 + l_y^2)]}{u_0}}.$$
(36)

The approximate solution of Eq. (29) is derived by applying the conservation of momentum [62,69,70], resulting in

$$E = \int_{-\infty}^{+\infty} \tilde{\Phi}^{(1)^2} d\tilde{\zeta} \quad \text{and} \quad \partial_T E = -2\nu E.$$
 (37)

From Eq. (35), we derive the approximate solution of the dZK equation in the following form

$$\tilde{\Phi}^{(1)}(\tilde{\zeta}) = \tilde{\Phi}_0^{(1)} \operatorname{sech}^2(\tilde{\zeta}/\tilde{L}). \tag{38}$$

Here, $\tilde{\Phi}_0^{(1)} = \Phi_0^{(1)}(T)$ and $\tilde{L} = L(T)$ represent the amplitude and width of the soliton, respectively, both dependent on time. By substituting Eq. (38) into Eq. (37), and applying the condition $\nu = 0$, we determine the amplitude and width of the soliton as defined by

$$\tilde{\Phi}_{0}^{(1)} = \frac{3\tilde{u}}{l_{z}A},$$

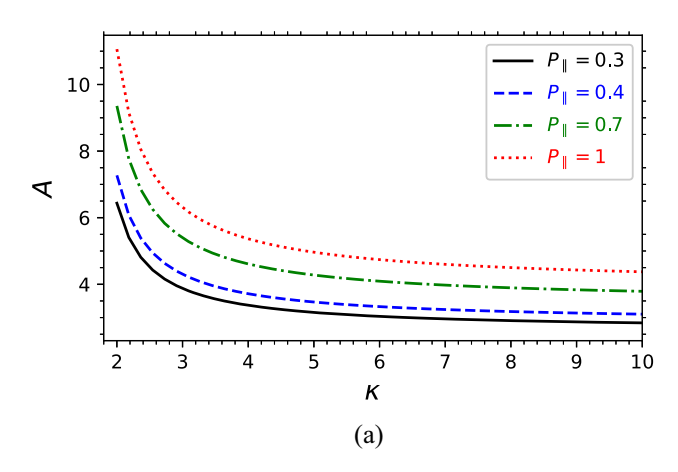
$$\tilde{L} = \sqrt{\frac{4l_{z}(B(l_{x}^{2} + l_{y}^{2}) + Cl_{z}^{2})}{\tilde{u}}},$$
(39)

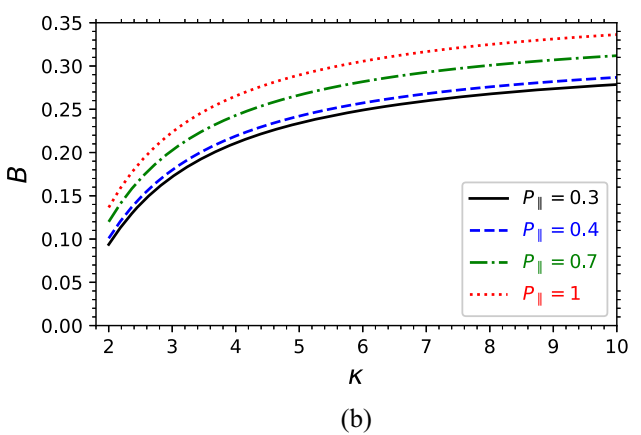
with $\tilde{u} = u_0 e^{-\nu T}$ and $\tilde{\zeta} = l_x X + l_y Y + l_z Z - \tilde{u} T$. Thus, the approximate solution of the dZK equation is:

$$\tilde{\Phi}^{(1)} = \frac{3u_0}{l_z A} e^{-\nu T} \operatorname{sech}^2 \left[\sqrt{\frac{u_0}{4l_z (B(l_x^2 + l_y^2) + Cl_z^2)}} e^{-\frac{\nu}{2}T} \tilde{\zeta} \right] \cdot (40)$$

4.2 Numerical analysis

In this section, we will numerically analyze the effects of plasma parameters on the occurrence and propagation of solitary waves in the plasma, specifically focusing on P_\perp , $P_{||}$, Ω_0 , and μ_p . Figure 10 presents the influence of superthermality on the coefficients A, B, and C for varying values of the parallel pressure component. We observe that for small values of the spectral parameter κ , A decreases while $P_{||}$ increases, B rises with κ and $P_{||}$, and C increases with κ but decreases with $P_{||}$. Superthermality diminishes the nonlinear effects, whereas anisotropy in pressure enhances the nonlinear effect. The medium exhibits increased dispersion with higher levels of superthermality. Like the parallel pressure component, the positron concentration exerts the same influence on nonlinearity (coefficient A)





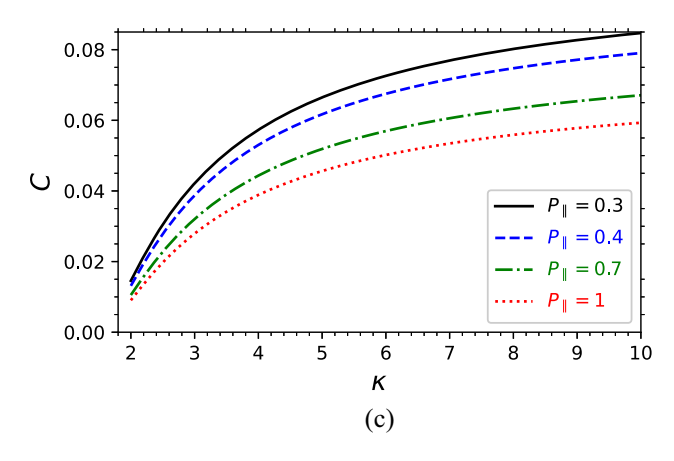


Figure 10: Variation of coefficient (a) A, (b) B, and (c) C against κ for different values of parallel component pressure $P_{||}$. Parameters fixed: $\omega_{ci}=0.4, \Omega_0=0.3, \sigma=1$, and $\mu_p=0.7$.

as P_{\parallel} (curve is not shown). The coefficients A and C are independent of the parameters P_{\perp} and Ω_0 , and the magnetic field, as indicated in Eq. (30). Figure 11 depicts the effect of the parallel (P_{\parallel}) and perpendicular (P_{\perp}) pressure components on the width of solitary waves propagating in the plasma. Figure 11(a) and (b) reveals that increasing anisotropy pressure leads to an increase in soliton width. This width also rises with the spectral parameter. For high

values of κ ($\kappa \to +\infty$), the soliton width tends to stabilize at a constant value. Anisotropy pressure thus increases the width of IASWs in this plasma model.

We recall that, unless otherwise stated, we have taken $l_x=0.3$, $l_y=0.5$, and $l_z=\sqrt{1-l_x^2-l_y^2}$. Figure 12 illustrates that in the absence of collisions ($\nu=0$), the amplitude of solitary waves decreases as the parallel pressure component P_{\parallel} and the electron–positron temperature ratio σ increase. Conversely, the amplitude increases with superthermality, eventually stabilizing as $\kappa\to +\infty$. Consequently, Maxwellian plasmas solitons exhibit higher amplitudes than those in superthermal plasmas. It is important to note that the coefficient A in Eq. (30) is unaffected by the perpendicular pressure component's soliton amplitude.

In the presence of collisions, the amplitude of the waves diminishes exponentially over time, as illustrated in Figure 13. The wave energy dissipates, leading the wave to become evanescent. This amplitude decreases with an increase in the parallel pressure component and increases with

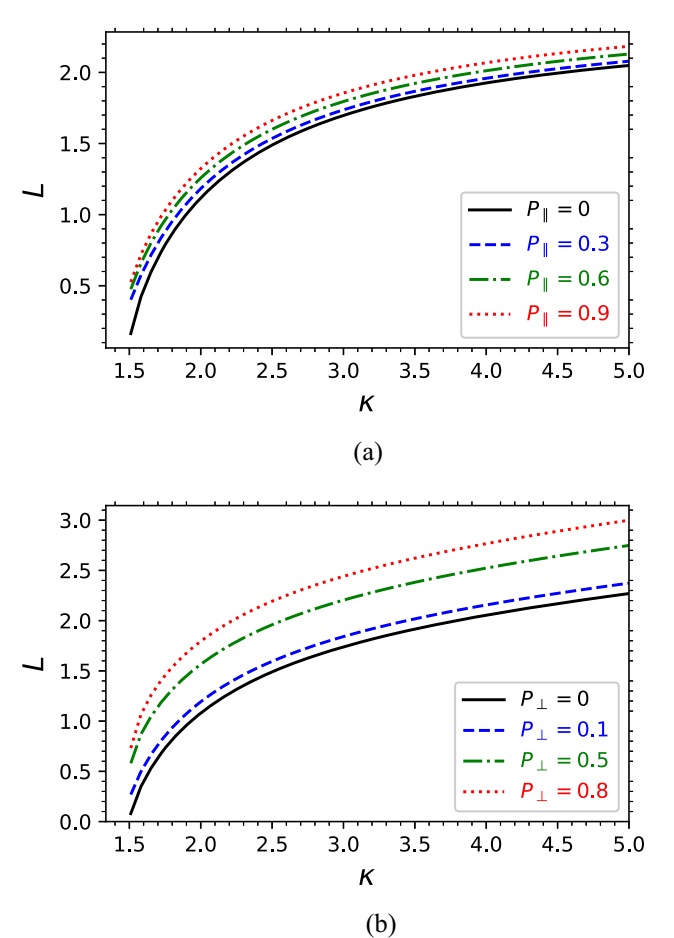
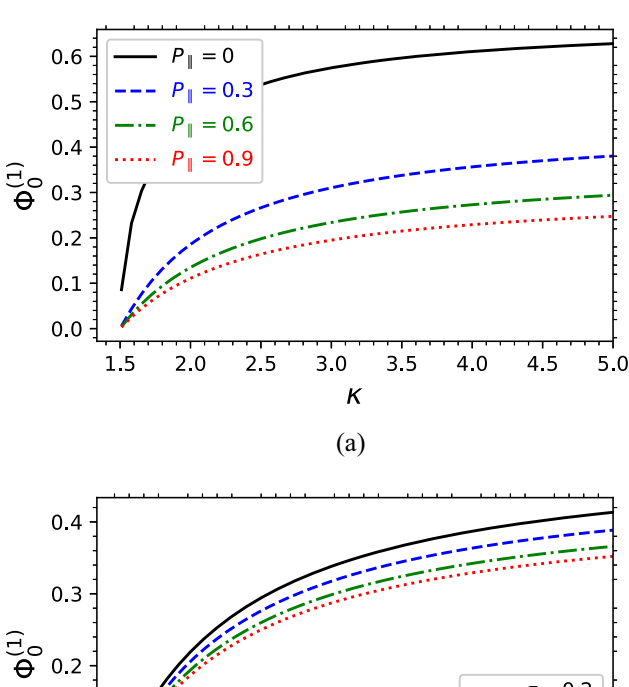


Figure 11: Variation of width L versus κ for different values of P_{\parallel} with $P_{\perp}=0.8$ (a) and P_{\perp} with $P_{\parallel}=0.01$ (b). Parameters fixed: $\mu_p=0.2$, $\sigma=0.2$, $\omega_{ci}=0.4$, $\Omega_0=0.05$, $u_0=0.3$, and v=0.



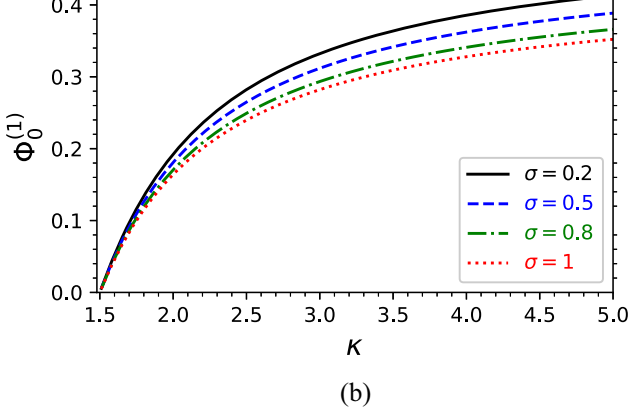


Figure 12: Variation of amplitude $\Phi_0^{(1)}$ versus κ for different values of $P_{||}$ with $\sigma=0.2$, $\mu_p=0.2$ (a) and σ with $P_{||}=0.6$, $\mu_p=0.2$ (b). Parameters fixed: $u_0=0.3$ and $\nu=0$.

superthermality κ . In the absence of collisions ($\nu=0$), we will now present the numerical study of the behavior of the parameters P_\perp , P_\parallel , κ , and Ω_0 on the electrostatic potential that characterizes the propagation of electrostatic waves in the plasma. Figure 14 illustrates the variations of the electrostatic potential $\Phi^{(1)}$ as a function of the independent variable ζ . Figure 14(a) reveals that for various values of superthermality κ , the amplitude and width of the soliton increase with rising values of the spectral parameter κ .

Superthermality decreases nonlinearity by enhancing the dispersion effect of the plasma. As $\kappa \to \infty$, the amplitude tends to a constant value. Figure 14(b) illustrates that for various values of the parallel component P_{\parallel} , the amplitude of IASWs decreases while the soliton width increases. Consequently, the parallel component of anisotropy pressure reduces wave amplitude and increases the width of these waves, making the plasma more nonlinear and dispersive. Therefore, increasing anisotropy pressure tends to lower the system's energy and stabilize the waves. Additionally, anisotropy pressure elevates the amplitude of

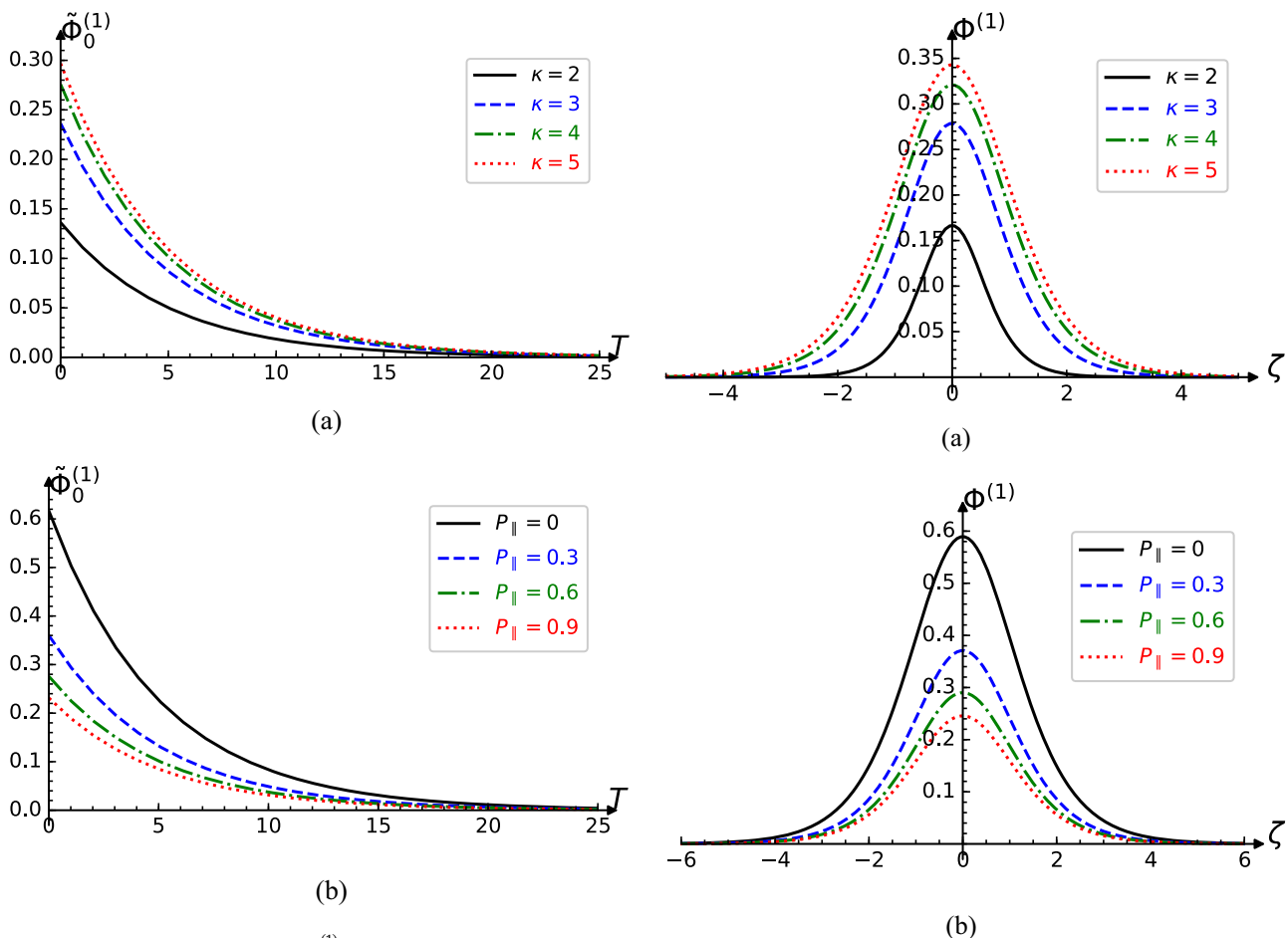


Figure 13: Variation of amplitude $\tilde{\Phi}_0^{(1)}$ versus T for different values of superthermality κ with $P_{||}$ = 0.6 (a) and parallel component pressure $P_{||}$ with κ = 4 (b). Parameters fixed: μ_p = 0.6, σ = 0.2, u_0 = 0.3 and ν = 0.4.

Figure 14: Plot electrostatic potential $\Phi^{(1)}$ against space variable ζ for different values of superthermality κ with $P_{\parallel}=0.3,\,\sigma=0.5,\,\mu_p=0.6$ (a) and parallel component pressure with $\kappa=5,\,\sigma=0.8,\,\mu_p=0.4$ (b) with other parameters fixed at: $\Omega_0=0.1,\,P_{\perp}=0.1,\,\mu_0=0.3,\,$ and $\omega_{ci}=0.4.$

solitary waves compared to superthermal plasma. Figure 15 illustrates the effect of the perpendicular pressure component P_{\perp} on the propagation of solitary waves. It shows that while the amplitude of electrostatic waves remains unchanged, the width of the waves increases. Thus, an increase in anisotropy pressure in the perpendicular component enhances the dispersiveness of the plasma medium while maintaining the nonlinear effect. Consequently, the waves propagate perpendicularly to the magnetic field with constant energy.

When considering the low rotation of the plasma with a frequency Ω_0 around the magnetic axis, known as the Coriolis effect, it is evident that as the frequency Ω_0 increases, the electrostatic waves maintain their amplitude while the soliton width decreases, resulting in a pointed, spiky soliton profile. This is depicted in Figure 16. This implies that the rotation of the plasma and its coupling effect with the magnetic field through ω_{ci} impact the dispersive properties of the wave profile. This finding aligns with the results of Farooq and Mushtaq [62]. When the

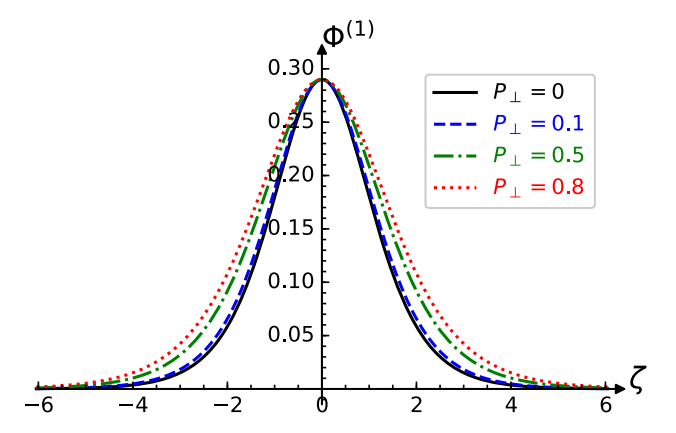


Figure 15: Plot electrostatic potential $\Phi^{(1)}$ against space variable ζ for different values of perpendicular component pressure P_{\perp} with other parameters fixed at: P_{\parallel} = 0.6, κ = 5, σ = 0.8, μ_p = 0.4, Ω_0 = 0.1, u_0 = 0.3, and ω_{ci} = 0.4.

parallel component of the magnetic field aligns with the rotation, leading particles to follow the field lines (strong field), the magnetic effect is amplified.

In a non-conservative plasma, dissipative solitons can form due to the balance between loss and gain terms, alongside the balance between dispersion and nonlinear effects. Additionally, the interaction between dispersion and dissipation effects can give rise to shock waves. In Figure 17, we illustrate the evolution of IASWs in the plasma by numerically plotting the solution of the ZK equation given in Eq. (40). Figure 17(a) demonstrates that in a non-collisional magnetized plasma ($\nu = 0$), the electrostatic waves maintain stability over time, with the amplitude and width of the soliton remaining constant as they propagate. Conversely, Figure 17(b) explores the solitary wave solution of Eq. (29) propagating in a collisional magnetized plasma ($\nu = 0.04$) in the absence of anisotropy pressure $(P_{\parallel} = P_{\perp} = 0)$ to highlight the effect of dissipation due to collisions. In this scenario, we observe that the amplitude of IASWs decreases while the width increases over time, all while conserving their fundamental properties. Figure 17(c) shows the combined effects of collisions and anisotropy pressure. We observe that coupling anisotropy pressure with collisions decreases the soliton amplitude by about twice as much as when considering the impact of collisions alone. The wave attenuates rapidly over time.

An increase in collision frequency results in the formation of a shorter and wider dissipative soliton in the magnetized e-p-i plasma. The soliton amplitude significantly decreases with rising collision frequency while the soliton width sharply increases, as shown in Figure 18. Based on the numerical results in Figure 18, it is observed that at higher collision frequencies compared to

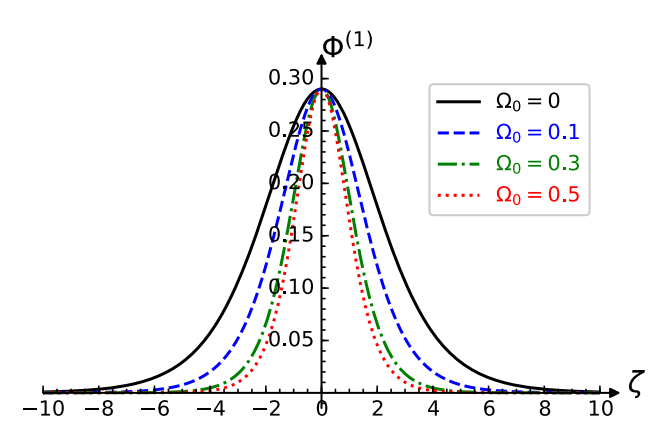


Figure 16: Plot electrostatic potential $\Phi^{(1)}$ against space variable ζ for different values of low frequency Ω_0 with other parameters fixed at: $P_{\parallel}=0.6, \kappa=5, \sigma=0.8, \mu_n=0.4, P_{\perp}=0.1, \mu_0=0.3, \text{ and } \omega_{ci}=0.4.$

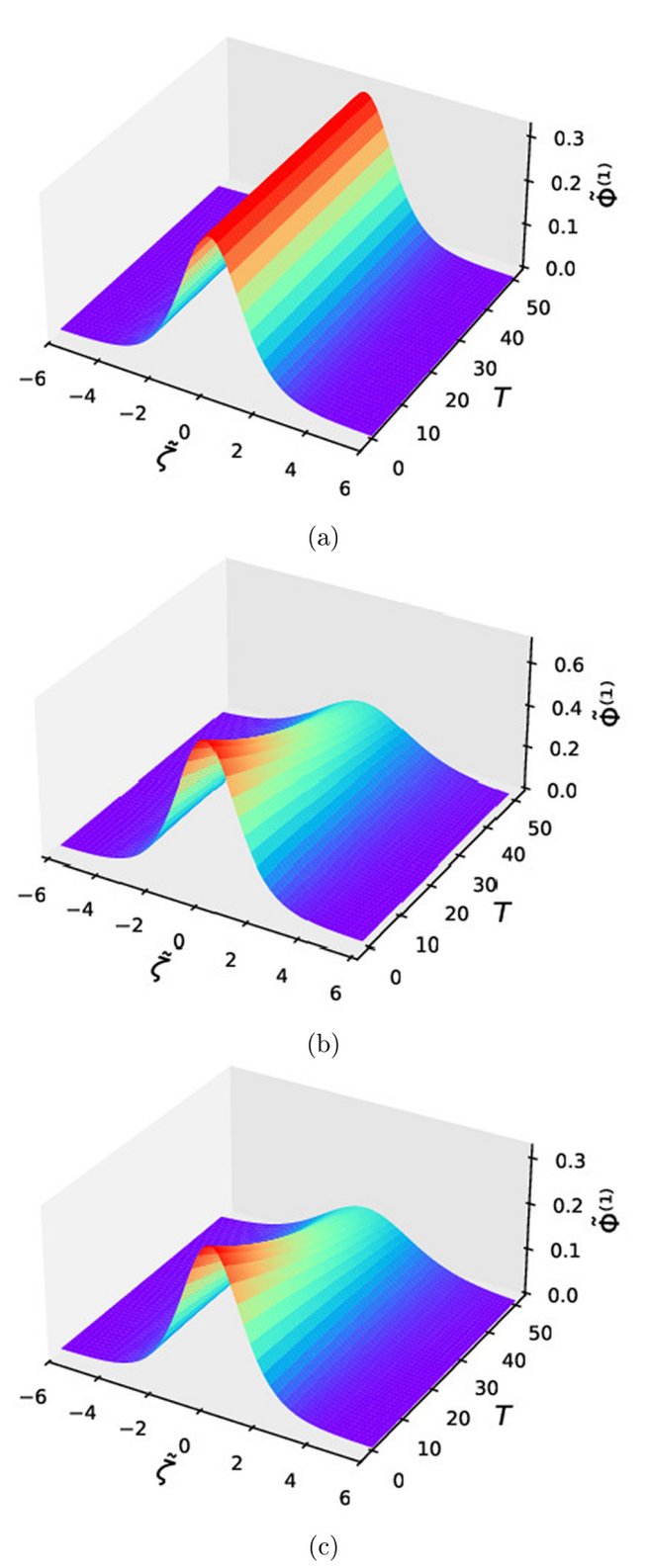


Figure 17: 3D plot of electrostatic potential $\tilde{\Phi}^{(1)}$ versus space variable $\tilde{\zeta}$ and time variable T with (a) $\nu=0$, $P_{\perp}=0.1$ and $P_{\parallel}=0.6$, (b) $\nu=0.04$ and $P_{\perp}=P_{\parallel}=0$ and (c) $\nu=0.04$, $P_{\perp}=0.1$ and $P_{\parallel}=0.6$. Parameters fixed: $\kappa=4$, $\mu_n=0.4$, $\sigma=0.2$, $\Omega=0.3$, $\omega_{ci}=0.4$, and $u_0=0.3$.

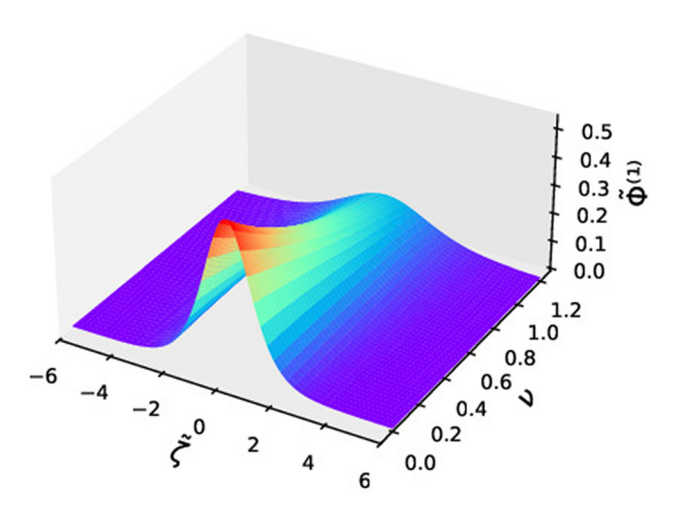


Figure 18: 3D plot of electrostatic potential $\tilde{\Phi}^{(1)}$ versus space variable $\tilde{\zeta}$ and collisional frequency ν . Parameters fixed: $\kappa=4$, $\mu_p=0.4$, $\sigma=0.2$, $\Omega=0.3$, $\omega_{ci}=0.4$, $P_\perp=0.1$, $P_\parallel=0.6$, T=2.2, and $u_0=0.5$.

dispersion, the formation of a shock wave in the magnetized e-p-i plasma can be expected.

5 Conclusion

In this study, we conducted analytical and numerical investigations into the linear and nonlinear propagation of electrostatic excitations within a collisional, magneto-rotating e-p-i plasma. This plasma is notable for its anisotropic ion pressure, ion collisions with neutrals, and the presence of superthermal electrons and positrons, characterized by a κ -distribution function. The anisotropic nature of the plasma is described by an asymmetric ion pressure tensor and is modeled using the CGL theory [22]. We have derived the dispersion equation, breaking it into components parallel and perpendicular to the magnetic field. The solution of this equation is expressed as a complex function, $(\omega = \omega_r + j\omega_{im})$. The oscillation of IAWs characterizes the parallel component, while the oscillation of electrostatic cyclotron waves characterizes the perpendicular component. The linear regime can be summarized as follows:

- 1) In the parallel component of the magnetic field in the dispersion relation:
 - a) We have demonstrated that there is a threshold wavenumber k_s , below which the real part of the frequency ω_r becomes imaginary, ($\omega_r^2 < 0$). This condition implies $k_s > k$ and $\omega_r = 0$ when k = 0, indicating the existence of IAWs.
 - b) The growth rate of the real frequency ω_r for ions increases with both superthermality κ and the

- wavenumber k. Consequently, ions exhibit instability at shorter wavelengths.
- c) The anisotropic pressure P_{\parallel} affects ion oscillations in this plasma model by increasing their frequency. A rise in P_{\parallel} leads to the instability of ion waves within the plasma.
- d) The real part ω_r of the ion frequency increases with the wavenumber k and decreases with both the electron–positron temperature ratio σ and the positron concentration μ_p . Consequently, an increase in positron concentration μ_p or a decrease in the positron temperature σ leads to a reduction in the frequency of ion oscillations, thereby stabilizing them.
- e) The imaginary part ω_{im} of the frequency is negative and decreases with increasing wavenumber k, indicating damped ion oscillations and the propagation of evanescent waves. The damping of oscillations is unaffected by σ , μ_p , and P_{\parallel} . However, the damping increases with rising collision frequency ν , as illustrated in Figure 3.
- f) We can predict that in the parallel component to the magnetic field, the waves propagate at the speed $v_p = \lim_{k \to 0} \frac{\omega_r}{k} = \left(\frac{1}{a_1} + P_{\parallel}\right)^{1/2}$.
- g) The collision frequency ν does not affect the wave propagation speed in the plasma.
- 2) In the perpendicular component of the magnetic field of the dispersion relation
 - a) For low collision frequencies $v \ll 1$, the frequency of ion oscillations is not zero when k=0. In this case, the frequency is approximately $\omega_r \approx \omega_{ci} + 2\Omega_0$, which characterizes the presence of electrostatic waves.
 - b) The growth rate of the frequency ω_r for ion oscillations on the phonon branch increases with the superthermality κ of the plasma and with the wavenumber. At infinite wavenumbers, ions become highly agitated and unstable due to their high frequency.
 - c) The frequency ω_r of oscillations increases with the wavenumber k and decreases with the positron concentration μ_p and the electron–positron temperature ratio σ . An increase in μ_p or σ stabilizes the ions. On the contrary, an increase in the plasma rotation frequency Ω_0 leads to a rise in the perturbation frequency of the ions. As shown in Figure 5(a), for short wavelengths (k > 1), the dispersion becomes linear, and the Coriolis effect diminishes due to the anisotropic nature of the plasma.

- d) The imaginary part ω_{im} of the perturbation frequency decreases as a function of the wavenumber k and remains consistently negative. It exhibits a transient regime and a steady-state regime. Numerical analysis indicates that increasing the positron concentration μ_p (or the electron–positron temperature ratio σ), as well as the plasma rotation frequency Ω_0 , causes the growth rate ω_{im} of the frequency to increase and approach zero, as shown in Figures 4(b) and 5(b). Additionally, the increase in the effect of the Coriolis force leads to a reduction in damped oscillations, thereby promoting wave propagation.
- d) Increasing the collision frequency v > 0 between ions and neutrals leads to a reduction in the growth rate $\omega_{im}(<0)$ of the frequency, which causes the damping of waves in the plasma, preventing propagation.
- e) The oscillation frequency ω_r increases with increasing anisotropic pressure P_\perp . This pressure anisotropy only affects waves at short wavelengths, where ions are highly excited and their frequency is proportional to the wavenumber $(\omega_r \propto k)$. Conversely, in the absence of pressure anisotropy $(P_\perp = 0)$ and as $k \to +\infty$, $\omega_r = 1$, indicating that ions reach a permanent oscillation regime with a constant frequency. In the dimensional case $(\omega_r \to \omega'/\omega_{pi})$, this constant frequency is the plasma frequency $(\omega' = \omega_{pi} (= \sqrt{4\pi Z_i n_{i0} e^2/m_i}))$. Note that an increase in the perpendicular pressure component P_\perp leads to the damping of waves in the medium.

The dZK equation, which models the evolution of IASWs, is derived using the RPM. The nonlinear and dispersion coefficients depend on various factors, including the κ index of superthermality, the parallel P_{\parallel} and perpendicular P_{\perp} pressure components, the plasma rotation frequency Ω_0 , the positron concentration μ_p , and the electron positron temperature ratio σ . The damping coefficient, however, remains constant and is solely dependent on the collision frequency ν . The summary of the nonlinear regime is as follows:

1) IAWs propagate in the plasma in a direction parallel to the magnetic field with a phase velocity that is unaffected by the plasma rotation frequency Ω_0 , the magnetic field through ω_{ci} , or the perpendicular pressure component P_{\perp} . The phase velocity increases with the κ index and parallel pressure P_{\parallel} and decreases with the temperature ratio σ .

- 2) The nonlinear effect increases with the parallel pressure component P_{\parallel} and decreases with higher values of the κ index of superthermality of electrons and positrons. In the parallel direction to the magnetic field, the dispersion effect decreases with the parallel pressure component P_{\parallel} and increases with the perpendicular pressure component P_{\perp} in the perpendicular direction to the magnetic field.
- 3) Ion pressure anisotropy has a significant impact on the amplitude and width of IASWs. The wave amplitude decreases with increasing ion pressure (P_{\parallel}) and the electron–positron temperature ratio (σ) . On the contrary, the amplitude increases with rising superthermality κ . As for soliton width, it increases with higher anisotropic pressure components $(P_{\perp} \text{ and } P_{\parallel})$. The higher the ion pressure, the more the solitary waves spread.
- 4) The Coriolis force, expressed through Ω_0 , exclusively affects the width of electrostatic waves. With increased plasma rotation, the width of the waves becomes narrower.
- 5) Collisions between ions and neutrals greatly affect the propagation properties of solitary waves in the plasma. Our analysis reveals that as the collision frequency ν increases, the medium becomes more strongly damped, resulting in an exponential decrease in the amplitude of solitary waves. Over time, the wave spreads while conserving its properties. When anisotropic pressure is combined with collisions, the soliton amplitude is reduced by approximately twice as much compared to the effect of collisions alone.
- 6) An increase in collision frequency results in a shorter and broader dissipative soliton in the magnetized e-p-i plasma.

In summary, our work offers a qualitative description of solitary wave observations in rotating space plasmas and astrophysical environments with high magnetic fields, such as the magnetosphere and the vicinity of Earth's magnetosheath, where nonthermal electrons and positrons coexist with anisotropic pressure ions.

6 Future work

In this study, the small-amplitude ion-acoustic dissipative solitons have been investigated by analyzing the damped ZK equation. Some discrepancies may appear between theoretical and practical observations, which requires some processing of the theoretical model to achieve complete agreement between theoretical results and experimental observations. To this end, in future works, we can follow the same work in the literature [71–75] by including the fifth-order dispersion in the governing equations to study the properties of large-amplitude dissipative nonlinear structures that can arise and propagate in the current plasma model or in any other model can describe by these equations. Additionally, the fractional calculus has played a vital role in recent times due to its ability to analyze various types of fractional evolutionary wave equations (EWEs) that can be used to model many different phenomena in many scientific disciplines [76-79]. Furthermore, studying the fractional EWEs is of great benefit in providing explanations for some unknown phenomena while studying these phenomena using the same EWEs in their integer forms. Therefore, in our future works, we intend to study the same current model in its fractional form to investigate the dynamics of propagation of the dissipative ion-acoustic solitary and cnoidal waves under the influence of fractionality. To do this, we will use the most recent methods discovered in analyzing fractional differential equations, such as the Tantawy technique and the new iterative method, and the residual power series method which have proven effective in many applications [80-84].

Acknowledgments: The authors express their gratitude to Princess Nourah bint Abdulrahman University Researchers Supporting Project Number (PNURSP2025R157), Princess Nourah bint Abdulrahman University, Riyadh, Saudi Arabia.

Funding information: The authors express their gratitude to Princess Nourah bint Abdulrahman University Researchers Supporting Project Number (PNURSP2025R157), Princess Nourah bint Abdulrahman University, Riyadh, Saudi Arabia. Also, this research work was funded by Institutional Fund Projects under grant no. (IFPIP: 981-247-1443). The authors gratefully acknowledge technical and financial support provided by the Ministry of Education and King Abdulaziz University, DSR, Jeddah, Saudi Arabia.

Author contributions: All authors have accepted responsibility for the entire content of this manuscript and approved its submission.

Conflict of interest: The authors state no conflict of interest.

Data availability statement: Data sharing does not apply to this article as no data sets were generated or analyzed during the current study.

References

- Popel SI, Vladimirov SV, Shukla PK. Ion-acoustic solitons in electron-positron-ion plasmas. Phys Plasmas. 1995;2:716.
- Nejoh YN. Effects of positron density and temperature on large amplitude ion-acoustic waves in an electron-positron-ion plasma. Austr | Phys. 1997;50:309.
- Nejoh YN. Large-amplitude ion-acoustic waves in a plasma with a relativistic electron beam. Phys Plasmas. 1996;3:1447.
- Hasegawa H, Irie S, Usami S, Ohsawa Y. Perpendicular nonlinear waves in an electron-positron-ion plasma. Phys Plasmas. 2002:9:2549.
- Mahmood S, Mushtaq A, Saleem H. Ion acoustic solitary wave [5] in homogeneous magnetized electron-positron-ion plasmas. New J Phys. 2003;5:28.
- Alrowaily AW, Khalid M, Kabir A, Salas AH, Tiofack CGL, Ismaeel SME, et al. On the Laplace new iterative method for modeling fractional positron-acoustic cnoidal waves in electronpositron-ion plasmas with Kaniadakis distributed electrons. Braz J Phys. 2025;55:106.
- Alrowaily AW, Khalid M, Kabir A, Tiofack CGL, Alhejaili W, Ismaeel SME, et al. On the electrostatic solitary waves in an electron-positron-ion plasma with Cairns-Tsallis distributed electrons. Rend Fis Acc Lincei. 2025;36:567-83. doi: 10.1007/s12210-025-01304-w.
- Almugrin AH, Alim, Mouhammadoul BB, Tiofack CGL, [8] Mohamadou A, Ismaeel SME, et al. Dromion structure in (2+1)dimensional modulated positron-acoustic waves in a non-Maxwellian magnetoplasma. Commun Theor Phys. 2025:77:055504.
- Alrowaily AW, Khalid M, Kabir A, Shah R, Tiofack CGL, Alhejaili W, et al. Arbitrary amplitude electron-acoustic solitary waves in magnetoplasma with Kaniadakis distributed electrons. AIP Adv. 2024;14:095324.
- [10] Washimi HR, Taniuti T. Propagation of ion-acoustic solitary waves of small amplitude. Phys Rev Lett. 1966;17:996.
- Sagdeev RZ. Reviews of plasma physics. Leontovich MA, editor, Consultants Bur., New York. Vol. 4. 1966. p. 23.
- Ikezi H, Tailor RJ, Baker DR. Formation and interaction of ionacoustic solitions. Phys Rev Lett. 1970;25:11.
- Almuqrin AH, Douanla DV, Tiofack CGL, Alim, Mohamadou A, Ismaeel SME, et al. On the propagation and interaction of the lowfrequency ion-acoustic multi-solitons in a magnetoplasma having nonextensive electrons using Hirota bilinear metho. J Low Frequency Noise Vibrat Active Control. 2025;44(3). doi: 10.1177/ 14613484251337289.
- [14] Hashmi T, Jahangir R, Masood W, Alotaibi BM, Ismaeel SME, El-Tantawy SA. Head-on collision of ion-acoustic (modified) Kortewegde Vries solitons in Saturn's magnetosphere plasmas with two temperature superthermal electrons. Phys Fluids. 2023;35:103104.
- [15] Shan SA. Coupled ion acoustic and drift solitons in a magnetized biion plasma with pseudo-potential approach. Phys Plasmas 2018;25:022113.
- [16] El-Sapa S, Becheikh N, Chtioui H, Lotfy K. Effects of variable thermal conductivity and magnetic field on the photo-thermoelastic wave propagation in hydro-microelongated semiconductor. Acta Mechanica. 2025;236:2509.
- [17] Ibrahim E, El-Sapa S, El-Bary AA, Lotfy K, Becheikh N, Chtioui H, et al. Moore-Gibson-Thompson model with the influence of

- moisture diffusivity of semiconductor materials during photothermal excitation. Front Phys. 2023;11:1224326.
- [18] Madhukalya B, Kalita J, Das R, Hosseini K, Baleanu D, Osman MS. Dynamics of ion-acoustic solitary waves in three-dimensional magnetized plasma with thermal ions and electrons: a pseudopotential analysis. Opt Quant Electron. 2024;56:898.
- [19] Madhukalya B, Kalita J, Das R, Hosseini K, Baleanu D, Osman MS. Small amplitude ion-acoustic solitary waves in a magnetized ionbeam plasma under the effect of ion and beam temperatures. Eur Phys J Plus. 2023;138:315.
- [20] Alhejaili W, Roy S, Raut S, Roy A, Salas AH, Aboelenen T, et al. Analytical solutions to (modified) Korteweg-de Vries-Zakharov-Kuznetsov equation and modeling ion-acoustic solitary, periodic, and breather waves in auroral magnetoplasmas. Phys Plasmas. 2024;31:082107.
- [21] Baumjohann W, Treumann RA. Basic Space Plasma Physics. London: Imperial College Press; 1997.
- [22] Chew GF, Goldberger ML, Low FE. The Boltzmann equation and the one-fluid hydromagnetic equations in the absence of particle collisions. Proc R Soc London A. 1956;236:112.
- [23] Parks GK. Physics of space plasmas. USA: Perseus; 1991.
- [24] Denton RE, Anderson BJ, Gary SP, Fuselier SA. Bounded anisotropy fluid model for ion temperatures. J Geophys Res. 1994;99:11.
- [25] Choi CR, Ryu C-M, Lee DY, Lee NC, Kim YH. Dust ion acoustic solitary waves in a magnetized dusty plasma with anisotropic ion pressure. Phys Lett A. 2007;364:297.
- [26] Gedalin M. Linear waves in relativistic anisotropic magnetohydrodynamics. Phys Rev E. 1993;47:6.
- [27] Gebretsadkan WB, Kalra GL. Propagation of linear waves in relativistic anisotropic magnetohydrodynamics. Phys Rev E. 2002;66:057401.
- [28] Adnan M, Mahmood S. Anisa Qamar. Small amplitude ion acoustic solitons in a weakly magnetized plasma with anisotropic ion pressure and kappa distributed electrons. Adv Space Res. 2014;53:845.
- [29] Chatterjee P, Saha T, Ryu C-M. Obliquely propagating ion acoustic solitary waves and double layers in a magnetized dusty plasma with anisotropic ion pressure. Phys Plasmas. 2008;15:123702.
- [30] Adnan M, Williams G, Qamar A, Mahmood S, Kourakis I. Pressure anisotropy effects on nonlinear electrostatic excitations in magnetized electron-positron-ion plasmas. Eur Phys J D. 2014;68:247.
- [31] Albalawi W, Hammad MA, Khalid M, Kabir A., Tiofack CGL, El-Tantawy SA. On the shock wave structures in anisotropy magnetoplasmas. AIP Adv. 2023;13:105309.
- [32] Irfan M, Ali S, El-Tantawy SA, Ismaeel SME. Three dimensional ionacoustic rogons in quantized anisotropic magnetoplasmas with trapped/untrapped electrons. Chaos. 2019;29:103133.
- [33] Douanla DV, Tiofack CGL, Alim A, Aboubakar M, Mohamadou A, Albalawi W, et al. Three-dimensional rogue waves and dustacoustic dark soliton collisions in degenerate ultradense magnetoplasma in the presence of dust pressure anisotropy. Phys Fluids. 2022;34:087105.
- [34] Almuqrin AH, Douanla DV, Tiofack CGL, Alim, Mohamadou A, Ismaeel SME, et al. Oblique collision of low-frequency dust-acoustic solitons and rogue waves in a multi-dimensional anisotropic self-gravitating electron-depleted complex plasmas. J Low Freq Noise Vib Act. 2025;44(1):207–29.
- [35] El-Sapa S, Alotaibi MA. Migration of two rigid spheres translating within an infinite couple stress fluid under the impact of magnetic field. Open Phys. 2024;22:20240085.

- [36] Vasyliunas VM. A survey of low-energy electrons in the evening sector of the magnetosphere with OGO 1 and OGO 3. J Geophys Res. 1968;73:2839.
- [37] Hasegawa A, Mima K, Duong-van M. Plasma distribution function in a superthermal radiation field. Phys Rev Lett. 1985;54:2608.
- [38] Pierrard V, Lemaire J, Lorentzian J. Lorentzian ion exosphere model. J Geophys Res. 1996;101:7923.
- [39] Pierrard V, Lamy H, Lemaire J. Exospheric distributions of minor ions in the solar wind. J Geophys Res. 2004;109:A02118.
- [40] Hellberg MA, Mace RL, Armstrong RJ, Karlstad G. Electron-acoustic waves in the laboratory: an experiment revisited. Phys Plasmas. 2000;64:433.
- [41] Goldman MV, Newman DL, Mangeney A. Theory of weak bipolar fields and electron holes with applications to space plasmas. Phys Rev Lett. 2007;99:145002.
- [42] Olsson A, Janhune P. Field-aligned conductance values estimated from Maxwellian and kappa distributions in quiet and disturbed events using Freia electron data. Ann Geophys. 1998;16:298.
- [43] Christon SP, Williams DJ, Mitchell DG, Frank LA, Huang Y. Spectral characteristics of plasma sheet ion and electron populations during disturbed geomagnetic conditions. J Geophys Res. 1989;94:13409.
- [44] Leubner MP, Vörös Z. A nonextensive entropy approach to solar wind intermittency. J Astrophys. 2005;618:547.
- [45] Shrauner BA, Feldman WC. Electromagnetic ion-cyclotron wave growth rates and their variation with velocity distribution function shape. J Plasma Phys. 1977;17:123.
- [46] Sultana S, Sarri S, Kourakis I. Electrostatic shock dynamics in superthermal plasmas. Phys Plasmas. 2012;19:012310.
- [47] Devanandhan S, Singh SV, Lakhina GS, Bharuthram R. Electron acoustic solitons in the presence of an electron beam and superthermal electrons. Nonlin. Process. Geophys. 2011;18:627.
- [48] Choi C-R, Min K-W, Rhee T-N. Electrostatic Korteweg-deVries solitary waves in a plasma with Kappa-distributed electrons. Phys Plasmas 2011;18:092901.
- [49] Shah A, Saeed R. Nonlinear Korteweg-de Vries-Burger equation for ion-acoustic shock waves in the presence of kappa distributed electrons and positrons. Plasma Phys Control Fusion. 2011;53:095006.
- [50] Saini NS, Kourakis I, Hellberg MA. Arbitrary amplitude ion-acoustic solitary excitations in the presence of excess superthermal electrons. Phys Plasmas. 2009;16:062903.
- [51] Sultana S, Kourakis I. Electrostatic solitary waves in the presence of excess superthermal electrons: modulational instability and envelope soliton modes. Plasma Phys Control Fusion. 2011;53:045003.
- [52] Sabry R, Moslem WM, Shukla PK. On the generation of envelope solitons in the presence of excess superthermal electrons and positrons. Astrophys Space Sci. 2011;333:203.
- [53] El-Tantawy SA, Wazwaz AM, Ata-ur Rahman. Three-dimensional modulational instability of the electrostatic waves in e-p-i magnetoplasmas having superthermal particles. Phys Plasmas. 2017:24:022126.
- [54] Singh SV, Devanandhan S, Lakhina GS, Bharuthram R. Effect of ion temperature on ion-acoustic solitary waves in a magnetized plasma in presence of superthermal electrons. Phys Plasmas. 2013:20:012306
- [55] Hussain S. The effect of spectral index parameter κ on obliquely propagating solitary wave structures in magneto-rotating plasmas. Chin Phys Lett. 2012;29:065202.

- [56] Chandrasekhar SS. The pressure in the interior of a star. Mon Not R Astron Soc. 1953;113:667.
- [57] Lehnert B. Magnetohydrodynamic waves under the action of the Coriolis force. Astrophys J. 1954;119:647.
- [58] Das GC, Nag A. Evolution of nonlinear ion-acoustic solitary wave propagation in rotating plasma. Phys Plasmas. 2006;13:082303.
- [59] Das GC, Nag A. Salient features of solitary waves in dusty plasma under the influence of Coriolis force. Phys Plasmas. 2007:14:083705
- [60] Moslem WM, Sabry R, Abdelsalam UM, Kourakis I, Shukla PK. Solitary and blow-up electrostatic excitations in rotating magnetized electron-positron-ion plasmas. New J Phys.
- [61] Hussain S, Akhtar N, Mahmood S. Ion acoustic solitary waves in electron-positron-ion magneto-rotating Lorentzian plasmas. Astrophys Space Sci. 2013;348:475.
- [62] Faroog M, Mushtag A, Qasim J. Dissipative ion acoustic solitary waves in collisional, magneto-rotating, non-thermal electronpositron-ion plasma. Contr Plasma Phys. 2019;59(1):122.
- [63] Xue J-K. Cylindrical and spherical ion-acoustic solitary waves with dissipative effect. Phys Lett A. 2004;322(3):225.
- [64] Purwins H-G, Bödeker HU, Amiranashvili S. Dissipative solitons. Adv Phys. 2010;59(5):485-701.
- [65] Chen FF. Introduction to Plasma Physics and Controlled Fusion, Cham: Springer; 62 (Los Angeles, CA 2015).
- [66] Ullah Khan S, Adnan M, Mahmood S Ur-Rehman H, Qamar A. Effect of pressure anisotropy on nonlinear periodic waves in a magnetized superthermal electron-positron-ion plasma. Brazilian J Phys. 2019;49:379-90.
- [67] Mugemana A, Lazarus IJ, Moolla S. Linear electrostatic waves in a three-component electron-positron-ion plasma. Phys Plasmas.
- [68] Williams G, Kourakis I. Nonlinear dynamics of multidimensional electrostatic excitations in nonthermal plasmas. Plasma Phys Control Fusion. 2013;55:055005.
- [69] Rakib HM, Sultana S. Damped dust-ion-acoustic solitons in collisional magnetized nonthermal plasmas. Contr Plasma Phys. 2021:61(9):e202100065.
- [70] Fedila Ali D, Djebli M. Small amplitude nonlinear electrostatic waves in a collisional complex plasma with positively charged dust. Phys Plasmas. 2010;17(10):102901.
- [71] El-Tantawy SA, Salas AH, Alyouse HA, Alharthi MR. Novel exact and approximate solutions to the family of the forced damped Kawahara equation and modeling strong nonlinear waves in a plasma. Chin J Phys. 2022;77:2454.
- [72] El-Tantawy SA, El-Sherif LS, Bakry AM, Alhejaili W, and Wazwaz A-M. On the analytical approximations to the nonplanar damped Kawahara equation: Cnoidal and solitary waves and their energy. Phys Fluids. 2022;34:113103.

- [73] Ismaeel SME, Wazwaz A-M, Tag-Eldin A-M, El-Tantawy SA. Simulation studies on the dissipative modified Kawahara solitons in a complex plasma. Symmetry. 2023;15(1):57.
- [74] Alyousef HA, Salas AH, Matoog RT, El-Tantawy SA. On the analytical and numerical approximations to the forced damped Gardner Kawahara equation and modeling the nonlinear structures in a collisional plasma. Phys Fluids. 2022:34:103105.
- [75] Aljahdaly NH, El-Tantawy SA. Novel anlytical solution to the damped Kawahara equation and its application for modeling the dissipative nonlinear structures in a fluid medium. J Ocean Eng Sci. 2022;7:492.
- [76] Az-Zo'bi EA, AlZoubi WA, Akinyemi L, Seno M, Alsaraireh IW, Mamat M. Abundant closed-form solitons for time-fractional integro-differential equation in fluid dynamics. Opt Quant Electron. 2021;53:132.
- [77] Az-Zo'bi EA, Alzoubi WA, Akinyemi L, Senol M, Masaedeh BS. A variety of wave amplitudes for the conformable fractional (2+1)dimensional Ito equation. Modern Phys Lett B. 2021;35(15):2150254.
- [78] Senol M, Gençyiqit M, Demirbilek U, Az-Zo'bi EA. Sensitivity and wave propagation analysis of the time-fractional (3+1)-dimensional shallow water waves model. Zeitschrift für angewandte Math Phys. 2024:75(3):78.
- [79] Abbas S, Inam I, Alharthi AM, AL-Khasawneh MAS, Az-Zo'bi EA, Garalleh HAL. Fractional magnetohydrodynamic Casson fluid flow with thermal radiation and buoyancy effects: a constant proportional Caputo model. Boundary Value Problems. 2025:2025:24
- [80] El-Tantawy SA, Al-Johani AS, Almuqrin AH, Khan A, El-Sherif LS. Novel approximations to the fourth-order fractional Cahn-Hillard equations: Application to the Tantawy Technique and other two techniques with Yang transform. J Low Frequency Noise Vibrat Active Control. 2025;44(3):1374-400. doi: 10.1177/ 14613484251322240.
- [81] El-Tantawy SA, Bacha SIH, Khalid M, Alhejaili W. Application of the Tantawy technique for modeling fractional ion-acoustic waves in electronegative plasmas having Cairns distributed-electrons, Part (I): Fractional KdV Solitary Waves. Braz J Phys. 2025;55:123.
- [82] El-Tantawy SA, Alhejaili W, Khalid M, Al-Johani AS. Application of the Tantawy technique for modeling fractional ion-acoustic waves in electronegative nonthermal Plasmas, Part (II): Fractional modifed KdV-solitary waves. Braz J Phys. 2025;55:176.
- [83] El-Tantawy SA, Khan D, Khan W, Khalid M, Alhejaili W. A novel approximation to the fractional KdV equation using the Tantawy technique and modeling fractional electron-acoustic Cnoidal waves in a nonthermal plasma. Braz J Phys. 2025;55:163.
- [84] Az-Zo'bi EA, Yildirim A, AlZoubi WA. The residual power series method for the one-dimensional unsteady flow of a van der Waals gas. Phys A Stat Mech Appl. 2019;517:188-96.